Journal of Computational Applied Mechanics 2025, 56(1): 43-68

DOI: 10.22059/jcamech.2024.380983.1192

RESEARCH PAPER

Hygro-thermo-mechanical bending of symmetric and asymmetric FGM Sandwich Plates with/without middle core Resting on Pasternak Foundation

Hiber Adem Mouloud Mohammed-Amine *, Beldjelili Youcef

Structures & Advances Materials Laboratory in Civil Engineering and Public Works, Faculty of Technology, Civil Engineering and Public Works Department, University of Sidi Bel Abbes, Algeria

Abstract

The bending of sandwich plates made of functionally graded material (FGM) that are supported by variable two-parameter elastic foundations under hygro-thermo-mechanical loads is covered in this paper. This study's methodology was based on refined trigonometric shear deformable plate theory (RTSDT) and four-variable refined plate theory. The governing equation was then obtained by introducing the virtual work principle and solving it using a Navier solution. We evaluated our intriguing results with several models found in the literature after we had obtained them. Lastly, we talked about the influence of the elastic foundation parameters, the plate aspect ratio, the power-law index, temperature and moisture differential, and the layer thickness ratio on symmetrical and asymmetrical plates, with or without a middle core.

Keywords: Functionally graded materials; Symmetrical sandwich plate; Asymmetrical sandwich plate; Middle core; Thermo-mechanical bending; Deflection and stress;

1. Introduction

Globally, sandwich structures are becoming increasingly common. The construction of sandwich is always needed in abundance due to its advantages, the emergence of new materials, and the need for high performance and lightweight building [1].

Among these new materials that are constantly being developed are functionally graded materials, which are advanced composites and can be used in various engineering constructions, such as construction of buildings, cars, aerospace, nuclear, ships and submarines [2].

We can describe functionally graded materials as composite materials of two types in particular so that the composition ratio of these materials is gradually variable towards the axis. This is a form of mixture that allows to

* Corresponding author.

E-mail address: adem.hiber@univ-sba.dz

exploit the advantages of both materials in an ideal and optional manner. One of the advantages of functionally graded materials is to maintain homogeneity [3].

The use of sandwich structures containing functional graded materials in plate making is highly suited by exploiting the gradual change towards thickness so that the physical characteristics of the facades and the interior of the plate are selected and this helps greatly because the two facades are regarded as an area of contact with external environment.

The plate receives several physical loads and often resting on elastic foundation. Winkler has proposed a model for this and then inserted Pasternak a shear layer as a parameter. This model is the best and most used in describing the mechanical behavior of structure-foundation interaction [4].

A large number of researchers and scientists have prioritized the study of these materials. We cite examples: Todd A. Anderson studied a sandwich composite with functionally graded core subjected to transverse loading by a rigid sphere employing an analytical three-dimensional elasticity solution method [5]. Abdelaziz, H.H. et al used displacement-based high-order shear deformation theory to investigate the static response of a functionally graded sandwich plate [6]. Q. Li et al conducted research The three-dimensional linear theory of elasticity is used to study the free vibration of sandwich rectangular plates with simply supported and clamped edges made of functionally graded material [7]. Keddouri, A. et al investigated a new displacement-based high-order shear deformation theory for the static response of functionally graded sandwich plates, with a new concept of porosity distribution that takes into consideration the composition and arrangement of the sandwich plate [8]. Merdaci, S and Mostefa, A.H studied an analytical solutions for the static and bending analysis of functionally graded sandwich plates with utilizing four-variable high order shear-deformation theory [9]. [1] Adhikari, B et al simulated the impact of a porosity type defect and examine the ramifications of porosity on the buckling properties of different kinds of FGM sandwich configurations [10]. Based on classical plate theory, Njim, E.K et al proposed a novel analytical method for performing the free vibration analysis of porous functionally graded (FG) sandwich plates (CPT) [11]. Scaled boundary finite element technique (SBFEM) is a semi-analytical tool used to examine the free vibration and transient dynamic behaviors of sandwich plates made of functionally graded material (FGM) by Liu, J et al [12]. Layerwise Theory was used by Sharma, N et al to analyze the vibration and uncertainty of a functionally graded sandwich plate [13]. An analytical model was developed by Georges, H. et al to calculate the stresses and deformations in sandwich panel graded lattice cores [14]. A comparison of finite element analysis and analytical methods for the bending of porous sandwich functionally graded material (FGM) plates was provided by Benameur, I. et al [15]. Timchenko, G. investigated the free vibration of porous power and sigmoid-law sandwich functionally graded (FG) plates with varying boundary conditions [16]. Using the finite element (FE) approach, Swaminathan, K. et al investigated the effects of porosity and localized edge stresses on the vibration and buckling characteristics of sandwich functionally graded material (FGM) plates [17]. A novel nth-order shear deformation theory was used by Vinh, P.V. to investigate the free vibration behavior of three-phase functionally graded sandwich plates [18]. Hadji, L. et al investigated the buckling and free vibration studies of multi-directional sandwich plates with functional grades and different boundary conditions [19]. Huang, Z. investigated the vibration behavior of soft-core sandwich plates with functionally graded materials under various boundary conditions [20].

Thermal deformations of sandwich plates made of functionally graded material (FGM) were studied in literature. Among them, Zenkour, A.M. et al used The sinusoidal shear deformation plate theory to study the thermal buckling of functionally graded material (FGM) sandwich plates [21]. Tounsi, A. et al took for the thermoelastic bending analysis of functionally graded sandwich plates, a refined trigonometric shear deformation theory (RTSDT) that includes transverse shear deformation effects into account is proposed [22]. In order to study a thermomechanical bending analysis of sandwich plates with functional grades, Benbakhti, A. et al introduced a novel quasi-3D type higher order shear deformation theory (HSDT) [23]. Li, D.et al considered A novel form of FGM sandwich plate subjected to thermomechanical bending study includes both FGM face sheets and FGM hard core [24]. Singh, S.J. et al used Galerkin Vlasov's method to study Thermo-mechanical analysis of porous sandwich S-FGM plate for different boundary conditions [25]. Daikh, A.A. et al. used a higher-order shear deformation plate theory to study the thermomechanical bending behavior of sandwich plates made of a completely ceramic core and functionally graded (FG) face sheets (HSDT) [26]. Using integral four-unknown shear deformation theory, Mahmoud, S.R. et al examined the thermomechanical bending response of porous functionally graded sandwich plates [27]. Han, M. et al studied Thermal Mechanical Bending Response of Symmetrical and Asymmetric Functionally Graded Material Plates [28, 29].

The bending of functionally graded sandwich plates under mechanical or thermomechanical strain, with or without elastic foundations, has been the subject of numerous investigations. The analysis of the hygro-thermo-mechanical bending response of symmetrical and asymmetric functionally graded material sandwich plates with and without a middle core resting on the Pasternak-Winkler foundation model is the case that has not been previously studied and is presented in this research paper. We applied the law of behavior of solids and the theory of refined shear deformation with formal functions for three distinct displacement fields in our investigation. Then, using the derived mathematical expressions, we applied the virtual works concept to arrive at a set of equations that we solved using the Navier solution. The effects of different parameters on the hygro-thermo-mechanical bending behavior of sandwich plates made of functionally graded material (FGM) resting on elastic foundations are illustrated with a few numerical examples.

2. Materials and Methods

Consider a rectangular FG sandwich plate with length a, width b and uniform thickness h, Layer 1, 2, 3 represent the bottom, middle and top layer, respectively.

The Cartesian coordinate system $x_1 x_2 x_3$ is taken such that the $x_1 x_2$ plane (x_3=0) coincides with the mid-plane of the sandwich plate.

The vertical ordinates of the bottom, the two interfaces, and the top are denoted by h_1 = −h/2, h_2, h_3, h_4 = h/2, respectively.

The combinations of three numbers, 1-0-1 for example, denote the thickness ratio in each layer from the bottom to the top as shown in Fig. 1.

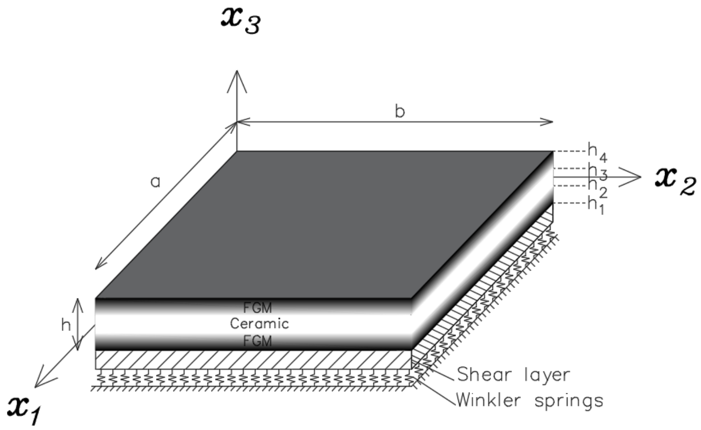

Fig 1: Geometry of a rectangular plate sandwiched by functionally graded material in Cartesian coordinates resting on Pasternak foundation.

The Voigt model helps describe the material properties of FGM as [30]:

$$\breve{p}(x_3) = \breve{p}_c \breve{V}_c(x_3) + \breve{p}_m \breve{V}_m(x_3) \tag{1}$$

where $\breve{p}_c$ and $\breve{p}_m$ represent the material properties (like Young's modulus, thermal expansion coefficient, moisture expansion coefficient etc.) of ceramics and metals, respectively.

$\breve{V}_c$ and $\breve{V}_m$ denote the volume fractions of ceramic and metal, respectively, with the constraint that $\breve{V}_c$ + $\breve{V}_m$ equals 1.

The volume fractions of metal are represented as:

$$\begin{cases} \breve{V}_m^{(1)}(x_3) = 1 - \left(\dfrac{x_3 - h_1}{h_2 - h_1}\right)^r; & x_3 \in [h_1, h_2] \\ \breve{V}_m^{(2)}(x_3) = 0; & x_3 \in [h_2, h_3] \\ \breve{V}_m^{(3)}(x_3) = 1 - \left(\dfrac{x_3 - h_4}{h_3 - h_4}\right)^r; & x_3 \in [h_3, h_4] \end{cases} \tag{2}$$

where r is the volume fraction index.

Based on the refined shear deformation plate theory, The displacement field can be expressed as follows [6]:

$$\begin{cases} X_1(x_1,x_2,x_3)=\breve{U}_0-x_3\dfrac{\partial \breve{W}_b}{\partial x_1}-\breve{f}(x_3)\dfrac{\partial \breve{W}_s}{\partial x_1} \\ X_2(x_1,x_2,x_3)=\breve{V}_0-x_3\dfrac{\partial \breve{W}_b}{\partial x_2}-\breve{f}(x_3)\dfrac{\partial \breve{W}_s}{\partial x_2} \\ X_3(x_1,x_2)=\breve{W}_b(x_1,x_2)+\breve{W}_s(x_1,x_2) \end{cases} \tag{3}$$

where $\breve{U}_0$ and $\breve{V}_0$ are the tensile parts in the x_1 and x_2 directions, respectively. $\breve{W}_b$ and $\breve{W}_s$ are the bending component and shearing component, respectively.

$\breve{f}(x_3)$ denotes the function in a way that determines the distribution of the transverse shear strains and stresses across the thickness of the plate.

For example, Reissner (1975) obtained the displacement of field by setting $\breve{f}(x_3)$ [31], and Reddy (1990) proposed the TSDPT by setting $\breve{f}(x_3)$ [32].

The displacement field for the CPT is obtained by setting $\breve{f}(x_3)=0$, and $\breve{f}(x_3)=x_3$ for the FSDT.

This research uses a shape function proposed by Touratier (1991) incorporating the trigonometric sine function which changes linearly through the plate thickness to predict the shear strain shown in following equation [33]:

$$\breve{f}(x_3)=x_3-\frac{h}{\pi}\sin\left(\frac{\pi x_3}{h}\right) \tag{4}$$

By employing small-strain elasticity theory and the displacement field, the strain components can be expressed as:

$$\begin{Bmatrix} \breve{\varepsilon}_{x_1} \\ \breve{\varepsilon}_{x_2} \\ \breve{\gamma}_{x_1x_2} \\ \breve{\gamma}_{x_2} \\ \breve{\gamma}_{x_1x_3} \end{Bmatrix} = \begin{Bmatrix} \dfrac{\partial X_1}{\partial x_1} \\ \dfrac{\partial X_2}{\partial x_2} \\ \dfrac{\partial X_2}{\partial x_1}+\dfrac{\partial X_1}{\partial x_2} \\ \dfrac{\partial X_3}{\partial x_2}+\dfrac{\partial X_2}{\partial x_3} \\ \dfrac{\partial X_3}{\partial x_1}+\dfrac{\partial X_1}{\partial x_3} \end{Bmatrix} \tag{5}$$

Substituting Equation (3) into Equation (5) gives:

$$\begin{Bmatrix} \breve{\varepsilon}_{x_1} \\ \breve{\varepsilon}_{x_2} \\ \breve{\gamma}_{x_1x_2} \\ \breve{\gamma}_{x_2x_3} \\ \breve{\gamma}_{x_1x_3} \end{Bmatrix} = \begin{Bmatrix} \breve{\varepsilon}^0_{x_1}+x_3\breve{k}^b_{x_1}+f\left(x_3\right)\breve{k}^s_{x_1} \\ \breve{\varepsilon}^0_{x_2}+x_3\breve{k}^b_{x_2}+\breve{f}\left(x_3\right)\breve{k}^s_{x_2} \\ \breve{\gamma}^0_{x_1x_2}+x_3\breve{k}^b_{x_1x_2}+\breve{f}\left(x_3\right)\breve{k}^s_{x_1x_2} \\ \breve{g}\left(x_3\right)\breve{\gamma}^s_{x_2x_3} \\ \breve{g}\left(x_3\right)\breve{\gamma}^s_{x_1x_3} \end{Bmatrix} \tag{6}$$

Where:

$$\left\{\breve{\varepsilon}^0\right\}=\begin{Bmatrix}\breve{\varepsilon}_{x_1}^0\\ \breve{\varepsilon}_{x_2}^0\\ \breve{\gamma}_{x_1x_2}^0\end{Bmatrix}=\begin{Bmatrix}\dfrac{\partial \breve{U}_0}{\partial x_1}\\ \dfrac{\partial \breve{V}_0}{\partial x_1}\\ \dfrac{\partial \breve{U}_0}{\partial x_2}+\dfrac{\partial \breve{V}_0}{\partial x_1}\end{Bmatrix},\left\{\breve{k}^b\right\}=\begin{Bmatrix}\breve{k}_{x_1}^b\\ \breve{k}_{x_2}^b\\ \breve{k}_{x_1x_2}^b\end{Bmatrix}=\begin{Bmatrix}-\dfrac{\partial^2 \breve{W}_b}{\partial {x_1}^2}\\ -\dfrac{\partial^2 \breve{W}_b}{\partial {x_2}^2}\\ -2\dfrac{\partial^2 \breve{W}_b}{\partial x_1\partial x_2}\end{Bmatrix},\left\{\breve{k}^s\right\}=\begin{Bmatrix}\breve{k}_{x_1}^s\\ \breve{k}_{x_2}^s\\ \breve{k}_{x_1x_2}^s\end{Bmatrix}=\begin{Bmatrix}-\dfrac{\partial^2 \breve{W}_s}{\partial {x_1}^2}\\ -\dfrac{\partial^2 \breve{W}_s}{\partial {x_2}^2}\\ -2\dfrac{\partial^2 \breve{W}_s}{\partial x_1\partial x_2}\end{Bmatrix}, \tag{7}$$

$$\left\{\breve{\gamma}^0\right\}=\begin{Bmatrix}\breve{\gamma}_{x_2x_3}^s\\ \breve{\gamma}_{x_1x_3}^s\end{Bmatrix}=\begin{Bmatrix}\dfrac{\partial \breve{W}_s}{\partial x_2}\\ \dfrac{\partial \breve{W}_s}{\partial x_1}\end{Bmatrix}$$

And:

$$\breve{g}\left(x_3\right)=1-\frac{d\breve{f}\left(x_3\right)}{dx_3}$$

The stress-strain relationships for a plane-stress state, incorporating hygro-thermal influences, can be expressed as follows [7]:

$$\begin{Bmatrix}\breve{\sigma}_{x_1}\\ \breve{\sigma}_{x_2}\\ \breve{\tau}_{x_1x_2}\\ \breve{\tau}_{x_2x_3}\\ \breve{\tau}_{x_1x_3}\end{Bmatrix}=\begin{bmatrix}\breve{C}_{11} & \breve{C}_{12} & 0 & 0 & 0\\ \breve{C}_{21} & \breve{C}_{22} & 0 & 0 & 0\\ 0 & 0 & \breve{C}_{44} & 0 & 0\\ 0 & 0 & 0 & \breve{C}_{55} & 0\\ 0 & 0 & 0 & 0 & \breve{C}_{66}\end{bmatrix}\begin{Bmatrix}\breve{\varepsilon}_{x_1}-\breve{\alpha}\left(x_3\right)\Delta\breve{T}-\breve{\beta}\left(x_3\right)\Delta\breve{C}\\ \breve{\varepsilon}_{x_2}-\breve{\alpha}\left(x_3\right)\Delta\breve{T}-\breve{\beta}\left(x_3\right)\Delta\breve{C}\\ \breve{\gamma}_{x_1x_2}\\ \breve{\gamma}_{x_2x_2}\\ \breve{\gamma}_{x_1x_3}\end{Bmatrix} \tag{8}$$

The $\breve{C}_{ij}$ expressions are given below:

$$\breve{C}_{11}=\breve{C}_{22}=\frac{\breve{E}\left(x_3\right)}{1-\breve{v}^2},\breve{C}_{12}=\breve{C}_{21}=\breve{v}\breve{C}_{11},\breve{C}_{44}=\breve{C}_{55}=\breve{C}_{66}=\frac{\breve{E}\left(x_3\right)}{2(1+\breve{v})}=\breve{C}_{33} \tag{9}$$

The modulus $\breve{E}(x_3)$, the thermal $\breve{\alpha}(x_3)$ and moisture expansion $\breve{\beta}(x_3)$ coefficients are variable relative to the depth of the plate as shown in the equation (01) $\breve{v}$ is poisson's ratio.

$\Delta\breve{T}$ and $\Delta\breve{C}$ are the temperature and humidity gradients through the thickness and are described in following equation as [34]

$$\Delta\breve{T}\left(x_1,x_2,x_3\right)=\breve{T}_1\left(x_1,x_2\right)+\frac{x_3}{h}\breve{T}_2\left(x_1,x_2\right)+\frac{1}{h}\breve{\Psi}\left(x_3\right)\breve{T}_3\left(x_1,x_2\right) \tag{10a}$$

$$\Delta\breve{C}\left(x_1,x_2,x_3\right)=\breve{C}_1\left(x_1,x_2\right)+\frac{x_3}{h}\breve{C}_2\left(x_1,x_2\right)+\frac{1}{h}\breve{\Psi}\left(x_3\right)\breve{C}_3\left(x_1,x_2\right) \tag{10b}$$

in which:

$$\breve{\Psi}(z)=\frac{h}{\pi}\sin\left(\frac{\pi x_3}{h}\right) \tag{11}$$

where $\breve{T}_1$, $\breve{T}_2$, $\breve{T}_3$ are the temperature loads and $\breve{C}_1$, $\breve{C}_2$, $\breve{C}_3$ are the humid environment loads.

Our FG sandwich plate resting on variable elastic foundations, and the density of reaction force of these foundations $\breve{f}_e$ can be expressed with following model:

$$\breve{f}_e = \breve{K}_w\left(x_1\right)X_3\left(x_1,x_2\right) - \breve{K}_G\nabla^2 X_3\left(x_1,x_2\right) \tag{12}$$

where $\breve{K}_w$ is Winkler parameter depended on x_1 only. It is considered to be linear, parabolic or sinusoidal as [35]:

$$\breve{K}_w\left(x_1\right) = \frac{\breve{J}_1 h^3}{a^4}\begin{cases} 1+\breve{\xi}\left(\dfrac{x_1}{a}\right) \\ 1+\breve{\xi}\left(\dfrac{x_1}{a}\right)^2 \\ 1+\breve{\xi}\sin\left(\pi\dfrac{x_1}{a}\right) \end{cases} \tag{13}$$

We consider $\breve{\xi} = 0$.

After setting the strain and the stress tensors, we use the principle of virtual work to generate the governing differential equations.

The principle applies the integral for the product of the stress and the variation of the strain in the x_1x_2 domain or Ω first and then integrates along the plate thickness as shown in equation (14).

$$\int_{-\frac{h}{2}}^{\frac{h}{2}}\int_\Omega\left[\breve{\sigma}_{x_1}\delta\breve{\varepsilon}_{x_1} + \breve{\sigma}_{x_2}\delta\breve{\varepsilon}_{x_2} + \breve{\tau}_{x_1x_2}\delta\breve{\gamma}_{x_1x_2} + \breve{\tau}_{x_2x_3}\delta\breve{\gamma}_{x_2x_3} + \breve{\tau}_{x_1x_3}\delta\breve{\gamma}_{x_1x_3}\right]d\Omega dz - \int_\Omega\left(\breve{q} - \breve{f}_e\right)\delta X_3 d\Omega = 0 \tag{14}$$

Substituting equation (6) and (8) into equation (14) and integrating across the thickness of the plate, equation (14) can be expressed as:

$$\begin{aligned}\int_\Omega\Big[&\breve{N}_{x_1}\delta\breve{\varepsilon}^0_{x_1} + \breve{N}_{x_1}\delta\breve{\varepsilon}^0_{x_2} + \breve{N}_{x_1x_2}\delta\breve{\gamma}^0_{x_1x_2} + \breve{M}^b_{x_1}\delta\breve{k}^b_{x_1} + \breve{M}^b_{x_2}\delta\breve{k}^b_{x_2} + \breve{M}^b_{x_1x_2}\delta\breve{k}^b_{x_1x_2} + \breve{M}^s_{x_1}\delta\breve{k}^s_{x_1} + \breve{M}^s_{x_2}\delta\breve{k}^s_{x_2} \\ &+\breve{M}^s_{x_1x_2}\delta\breve{k}^s_{x_1x_2} + \breve{S}^s_{x_2x_3}\delta\breve{\gamma}^s_{x_2x_3} + \breve{S}^s_{x_1x_3}\delta\breve{\gamma}^s_{x_1x_3}\Big]d\Omega - \int_\Omega\left(\breve{q} - \breve{f}_e\right)\delta\breve{W}d\Omega\end{aligned} \tag{15}$$

the stress resultants $\breve{N}$, $\breve{M}$, and $\breve{S}$ are expressed as:

$$\begin{Bmatrix}\{\breve{N}\} \\ \{\breve{M}^b\} \\ \{\breve{M}^s\}\end{Bmatrix} = \begin{Bmatrix}\breve{N}_{x_1}, \breve{N}_{x_2}, \breve{N}_{x_1x_2} \\ \breve{M}^b_{x_1}, \breve{M}^b_{x_2}, \breve{M}^b_{x_1x_2} \\ \breve{M}^s_{x_1}, \breve{M}^s_{x_1}, \breve{M}^s_{x_1x_2}\end{Bmatrix} = \sum_{n=1}^{3}\int_{h_{n-1}}^{h_n}\left(\breve{\sigma}_{x_1}, \breve{x}_{x_2}, \breve{\tau}_{x_1x_2}\right)^n\begin{Bmatrix}1 \\ x_3 \\ \breve{f}\left(x_3\right)\end{Bmatrix}dx_3 \tag{16a}$$

$$\left\{\breve{S}^s\right\} = \left(\breve{S}^s_{x_2x_3}, \breve{S}^s_{x_1x_3}\right) = \sum_{n=1}^{3}\int_{h_{n-1}}^{h_n}\left(\breve{\tau}_{x_2x_3}, \breve{\tau}_{x_1x_3}\right)^n\breve{g}\left(x_3\right)dx_3 \tag{16b}$$

where h_n and h_{n-1} are the top and bottom x_3-coordinates of the nth layer.

Substituting equation (6) into equation (8) and the subsequent results into equation (16), the stress resultants can be expressed as:

$$\begin{Bmatrix}\{\breve{N}\} \\ \{\breve{M}^b\} \\ \{\breve{M}^s\}\end{Bmatrix} = \begin{bmatrix}[\breve{A}] & [\breve{B}] & [\breve{B}^s] \\ [\breve{B}] & [\breve{D}] & [\breve{D}^s] \\ [\breve{B}^s] & [\breve{D}^s] & [\breve{H}^s]\end{bmatrix}\begin{Bmatrix}\{\breve{\varepsilon}^0\} \\ \{\breve{k}^b\} \\ \{\breve{k}^s\}\end{Bmatrix} - \begin{Bmatrix}\{\breve{N}^T\} \\ \{\breve{M}^{bT}\} \\ \{\breve{M}^{sT}\}\end{Bmatrix} - \begin{Bmatrix}\{\breve{N}^C\} \\ \{\breve{M}^{bC}\} \\ \{\breve{M}^{sC}\}\end{Bmatrix}, \left\{\breve{S}^s\right\} = \left[\breve{A}^s\right]\left\{\breve{\gamma}^0\right\} \tag{17}$$

Where:

$$\breve{A}_{ij}, \breve{B}_{ij}, \breve{D}_{ij}, \breve{B}^s_{ij}, \breve{D}^s_{ij}, \breve{H}^s_{ij} = \sum_{n=1}\int_{h_{n-1}}^{h_n}\breve{C}^n_{ij}\left(1, x_3, x_3{}^2, \breve{f}\left(x_3\right), x_3\breve{f}\left(x_3\right), \breve{f}\left(x_3\right)^2\right)dx_3, (i, j = 1,2,3) \tag{18a}$$

$$\breve{A}^s_{ij} = \sum_{n=1}^{3}\int_{h_{n-1}}^{h_n}\breve{C}^n_{33}\left(\breve{g}\left(x_3\right)\right)^2 dx_3, (i, j) = 1,2 \tag{18b}$$

$$\left\{\breve{N}^{T,C}\right\}=\begin{Bmatrix}\breve{N}_{x_1}^{T,C}\\ \breve{N}_{x_2}^{T,C}\\ 0\end{Bmatrix},\left\{\breve{M}^{bT,bC}\right\}=\begin{Bmatrix}\breve{M}_{x_1}^{bT,bC}\\ \breve{M}_{x_2}^{bT,bC}\\ 0\end{Bmatrix},\left\{\breve{M}^{sT,sC}\right\}=\begin{Bmatrix}\breve{M}_{x_1}^{sT,sC}\\ \breve{M}_{x_2}^{sT,sC}\\ 0\end{Bmatrix} \tag{18c}$$

The resultant hygrothermal forces $\breve{N}_{x_1}^{T,C}=\breve{N}_{x_2}^{T,C},\breve{M}_{x_1}^{bT,bC}=\breve{M}_{x_2}^{bT,bC},\breve{M}_{x_1}^{sT,sC}=\breve{M}_{x_2}^{sT,sC}$ are expressed by:

$$\left[\breve{N}_{x_1}^{T}\quad,\breve{M}_{x_1}^{bT}\quad,\breve{M}_{x_1}^{sT}\right]=\sum_{n=1}^{3}\int_{h_{n-1}}^{h_n}\frac{\breve{E}^{(n)}\left(x_3\right)}{1-\breve{\nu}}\left[1\quad,x_3\quad,\breve{f}\left(x_3\right)\right]\breve{\alpha}^{(n)}\left(x_3\right)\Delta\breve{T}dx_3 \tag{19a}$$

$$\left[\breve{N}_{x_1}^{C}\quad,\breve{M}_{x_1}^{bC}\quad,\breve{M}_{x_1}^{sC}\right]=\sum_{n=1}^{3}\int_{h_{n-1}}^{h_n}\frac{\breve{E}^{(n)}\left(x_3\right)}{1-\breve{\nu}}\left[1\quad,x_3\quad,\breve{f}\left(x_3\right)\right]\breve{\beta}^{(n)}\left(x_3\right)\Delta\breve{C}dx_3 \tag{19b}$$

The equilibrium equations governing the systeme can be obtained from equation (15) through the integration of displacement gradients by parts, with the subsequent step of setting each coefficient to zero separately.

In this manner, one can obtain the equilibrium equations corresponding to the current theory as:

$$\begin{aligned}
&\delta\breve{U}_0:\frac{\partial\breve{N}_{x_1}}{\partial x_1}+\frac{\partial\breve{N}_{x_1x_2}}{\partial x_1x_2}=0\\
&\delta\breve{V}_0:\frac{\partial\breve{N}_{x_1x_2}}{\partial x_1}+\frac{\partial\breve{N}_{x_2}}{\partial x_2}=0\\
&\delta\breve{W}_b:\frac{\partial^2\breve{M}_{x_1}^{b}}{\partial x_1^{\,2}}+2\frac{\partial^2\breve{M}_{x_1x_2}^{b}}{\partial x_1\partial x_2}+\frac{\partial^2\breve{M}_{x_2}^{b}}{\partial x_2^{\,2}}-\breve{f}_e+\breve{q}=0\\
&\delta\breve{W}_b:\frac{\partial^2\breve{M}_{x_1}^{s}}{\partial x_1^{\,2}}+2\frac{\partial^2\breve{M}_{x_1x_2}^{s}}{\partial x_1\partial x_2}+\frac{\partial^2\breve{M}_{x_1}^{s}}{\partial x_2^{\,2}}+\frac{\partial\breve{S}_{x_1x_3}^{s}}{\partial x_1}+\frac{\partial\breve{S}_{x_2x_3}^{s}}{\partial x_2}-\breve{f}_e+\breve{q}=0
\end{aligned} \tag{20}$$

The equilibrium equations governing the system can be formulated with respect to displacements ($\breve{U}_0,\breve{V}_0,\breve{W}_b,\breve{W}_s$) as outlined below:

$$\begin{aligned}
&\breve{A}_{11}d_{11}\breve{U}_0+\breve{A}_{66}d_{22}\breve{U}_0+\left(\breve{A}_{12}+\breve{A}_{66}\right)d_{12}\breve{V}_0-\breve{B}_{11}d_{111}\breve{W}_b-\left(\breve{B}_{12}+2\breve{B}_{66}\right)d_{122}\breve{W}_b\\
&-\left(\breve{B}_{12}^s+2\breve{B}_{66}^s\right)d_{122}\breve{W}_s-\breve{B}_{11}^s d_{111}\breve{W}_s=\breve{p}_1
\end{aligned} \tag{21a}$$

$$\begin{aligned}
&\breve{A}_{22}d_{22}\breve{V}_0+\breve{A}_{66}d_{11}\breve{V}_0+\left(\breve{A}_{12}+\breve{A}_{66}\right)d_{12}\breve{U}_0-\breve{B}_{22}d_{222}\breve{W}_b-\left(\breve{B}_{12}+2\breve{B}_{66}\right)d_{112}\breve{W}_b\\
&-\left(\breve{B}_{12}^s+2\breve{B}_{66}^s\right)d_{112}\breve{W}_s-\breve{B}_{22}^s d_{222}\breve{W}_s=\breve{p}_2
\end{aligned} \tag{21b}$$

$$\begin{aligned}
&\breve{B}_{11}d_{111}\breve{U}_0+\left(\breve{B}_{12}+2\breve{B}_{66}\right)d_{122}\breve{U}_0+\left(\breve{B}_{12}+2\breve{B}_{66}\right)d_{112}\breve{V}_0+\breve{B}_{22}d_{222}\breve{V}_0-\breve{D}_{11}d_{1111}\breve{W}_b\\
&-2\left(\breve{D}_{12}+2\breve{D}_{66}\right)d_{1122}\breve{W}_b-\breve{D}_{22}d_{2222}\breve{W}_b-\breve{D}_{11}^s d_{1111}\breve{W}_s-2\left(\breve{D}_{12}^s+2\breve{D}_{66}^s\right)d_{1122}\breve{W}_s\\
&-\breve{D}_{22}^s d_{2222}\breve{W}_s=\breve{p}_3
\end{aligned} \tag{21c}$$

$$\breve{B}_{11}^{s}d_{111}\breve{U}_{0}+\left(\breve{B}_{12}^{s}+2\breve{B}_{66}^{s}\right)d_{122}\breve{U}_{0}+\left(\breve{B}_{12}^{s}+2\breve{B}_{66}^{s}\right)d_{112}\breve{V}_{0}+\breve{B}_{22}^{s}d_{222}\breve{V}_{0}-\breve{D}_{11}^{s}d_{1111}\breve{W}_{b}$$
$$-2\left(\breve{D}_{12}^{s}+2\breve{D}_{66}^{s}\right)d_{1122}\breve{W}_{b}-\breve{D}_{22}^{s}d_{2222}\breve{W}_{b}-\breve{H}_{11}^{s}d_{1111}\breve{W}_{s}-2\left(\breve{H}_{12}^{s}+2\breve{H}_{66}^{s}\right)d_{1122}\breve{W}_{s} \quad (21d)$$
$$-\breve{H}_{22}^{s}d_{2222}\breve{W}_{s}+\breve{A}_{55}^{s}d_{11}\breve{W}_{s}+\breve{A}_{44}^{s}d_{22}\breve{W}_{s}=\breve{p}_{4}$$

where d_i, d_{ij}, d_{ijl} *and* d_{ijlm} are the following differential operators:

$$d_i=\frac{\partial}{\partial x_i},d_{ij}=\frac{\partial^2}{\partial x_i\partial x_j},d_{ijl}=\frac{\partial^3}{\partial x_i\partial x_j\partial x_l},d_{ijlm}=\frac{\partial^4}{\partial x_i\partial x_j\partial x_l\partial x_m},\quad (i,j,l,m=1,2) \quad (22)$$

The elements of the generalized force vector $\{p\}$ are provided by:

$$\breve{p}_1=\frac{\partial\breve{N}_{x_1}^{T}}{\partial x_1}+\frac{\partial\breve{N}_{x_1}^{C}}{\partial x_1},\breve{p}_2=\frac{\partial\breve{N}_{x_2}^{T}}{\partial x_2}+\frac{\partial\breve{N}_{x_2}^{C}}{\partial x_2},$$
$$\breve{p}_3=\breve{f}_e-\breve{q}+\frac{\partial^2\left(\breve{M}_{x_1}^{bT}+\breve{M}_{x_1}^{bC}\right)}{\partial x_1{}^2}+\frac{\partial^2\left(\breve{M}_{x_2}^{bT}+\breve{M}_{x_2}^{bC}\right)}{\partial x_2{}^2}, \quad (23)$$
$$\breve{p}_4=\breve{f}_e-\breve{q}+\frac{\partial^2\left(\breve{M}_{x_1}^{sT}+\breve{M}_{x_1}^{sC}\right)}{\partial x_1{}^2}+\frac{\partial^2\left(\breve{M}_{x_2}^{sT}+\breve{M}_{x_2}^{sC}\right)}{\partial x_2{}^2}$$

For resolving the equation (21) in the case of a simply supported rectangular plate with length a and width b.

The Navier method is used in this paper, he considered the mechanical, temperature and moisture loads, $\breve{q}$, $\breve{T}_i$ and $\breve{C}_i$ in the form of a double Fourier series as:

$$\begin{Bmatrix}\breve{q}\\ \breve{T}_i\\ \breve{C}_i\end{Bmatrix}=\begin{Bmatrix}\breve{q}_0\\ \breve{t}_i\\ \breve{c}_i\end{Bmatrix}\sin\left(\lambda x_1\right)\sin\left(\mu x_2\right),(i=1,2,3) \quad (24)$$

where $\breve{q}_0$, $\breve{t}_1$, $\breve{t}_2$, $\breve{t}_3$, $\breve{c}_1$, $\breve{c}_2$ and $\breve{c}_3$ are constants, λ and μ are given by:

$$\lambda=\frac{\pi}{a},\mu=\frac{\pi}{b} \quad (25)$$

The Navier method is used to obtain the analytical solution. Displacements in the midplane are represented by constants (U, V, W_b, W_s), which are then multiplied by sine and cosine functions to meet the conditions imposed by the boundaries of the simply supported plates.

$$\begin{Bmatrix}\breve{U}_0\\ \breve{V}_0\\ \breve{W}_b\\ \breve{W}_s\end{Bmatrix}=\begin{Bmatrix}\tilde{X}_1\cos(\lambda x)\sin(\mu y)\\ \tilde{X}_2\sin(\lambda x)\cos(\mu y)\\ \tilde{X}_3^b\sin(\lambda x)\sin(\mu y)\\ \tilde{X}_3^s\sin(\lambda x)\sin(\mu y)\end{Bmatrix} \quad (26)$$

Currently, the assumed forms of the loads and middle plane displacements are inserted into the governing differential equations, yielding the subsequent system of equations:

$$[\breve{K}]\{\Delta\}=\{\breve{P}\} \quad (27)$$

the vector $\{\Delta\}$ represents the displacement coefficients ($\tilde{X}_1$, $\tilde{X}_1$, $\tilde{X}_3^b$, $\tilde{X}_3^s$) and $[\breve{K}]$ the symmetric matrix is expressed as:

$$[\breve{K}]=\begin{bmatrix}\breve{k}_{11}&\breve{k}_{12}&\breve{k}_{13}&\breve{k}_{14}\\ \breve{k}_{12}&\breve{k}_{22}&\breve{k}_{23}&\breve{k}_{24}\\ \breve{k}_{13}&\breve{k}_{23}&\breve{k}_{33}&\breve{k}_{34}\\ \breve{k}_{14}&\breve{k}_{24}&\breve{k}_{34}&\breve{k}_{44}\end{bmatrix} \quad (28)$$

Where:

$$
\begin{aligned}
&\breve{k}_{11}=-\left(\breve{A}_{11}\lambda^2+\breve{A}_{66}\mu^2\right),\breve{k}_{12}=-\lambda\mu\left(\breve{A}_{12}+\breve{A}_{66}\right),\breve{k}_{13}=\lambda\left[\breve{B}_{11}\lambda^2+\left(\breve{B}_{12}+2\breve{B}_{66}\right)\mu^2\right],\\
&\breve{k}_{14}=\lambda\left[\breve{B}^s_{11}\lambda^2+\left(\breve{B}^s_{12}+2\breve{B}^s_{66}\right)\mu^2\right],\\
&\breve{k}_{22}=-\left(\breve{A}_{66}\lambda^2+\breve{A}_{22}\mu^2\right),\breve{k}_{23}=\mu\left[\left(\breve{B}_{12}+2\breve{B}_{66}\right)\lambda^2+\breve{B}_{22}\mu^2\right],\\
&\breve{k}_{24}=\mu\left[\left(\breve{B}^s_{12}+2\breve{B}^s_{66}\right)\lambda^2+\breve{B}^s_{22}\mu^2\right],\\
&\breve{k}_{33}=-\left(\breve{D}_{11}\lambda^4+2\left(\breve{D}_{12}+2\breve{D}_{66}\right)\lambda^2\mu^2+\breve{D}_{22}\mu^4+\bar{\breve{K}}_w+\breve{K}_G\left(\lambda^2+\mu^2\right)\right),\\
&\breve{k}_{34}=-\left(\breve{D}^s_{11}\lambda^4+2\left(\breve{D}^s_{12}+2\breve{D}^s_{66}\right)\lambda^2\mu^2+\breve{D}^s_{22}\mu^4+\bar{\breve{K}}_w+\breve{K}_G\left(\lambda^2+\mu^2\right)\right),\\
&\breve{k}_{44}=-\left(\breve{H}^s_{11}\lambda^4+2\left(\breve{H}^s_{11}+2\breve{H}^s_{66}\right)\lambda^2\mu^2+\breve{H}^s_{22}\mu^4+\breve{A}^s_{55}\lambda^2+\breve{A}^s_{44}\mu^2+\bar{\breve{K}}_w+\breve{K}_G\left(\lambda^2+\mu^2\right)\right)
\end{aligned}
\tag{29}
$$

and the components of the generalized force vector $\{\breve{P}\}$ =?? $\breve{P}_1$, $\breve{P}_2$, $\breve{P}_3$, $\breve{P}_4$?? are expressed by:

$$
\begin{aligned}
&\breve{P}_1=\lambda\left[\left(\breve{A}^T\breve{t}_1+\breve{B}^T\breve{t}_2+{}^a\breve{B}^T\breve{t}_3\right)+\left(\breve{A}^C\breve{c}_1+\breve{B}^C\breve{c}_2+{}^a\breve{B}^C\breve{c}_3\right)\right],\\
&\breve{P}_2=\mu\left[\left(\breve{A}^T\breve{t}_1+\breve{B}^T\breve{t}_2+{}^a\breve{B}^T\breve{t}_3\right)+\left(\breve{A}^C\breve{c}_1+\breve{B}^C\breve{c}_2+{}^a\breve{B}^C\breve{c}_3\right)\right],\\
&\breve{P}_3=-\breve{q}_0-h\left(\lambda^2+\mu^2\right)\left[\left(\breve{B}^T\breve{t}_1+\breve{D}^T\breve{t}_2+{}^a\breve{D}^T\breve{t}_3\right)+\left(\breve{B}^C\breve{c}_1+\breve{D}^C\breve{c}_2+{}^a\breve{D}^C\breve{c}_3\right)\right],\\
&\breve{P}_4=-\breve{q}_0-h\left(\lambda^2+\mu^2\right)\left[\left({}^s\breve{B}^T\breve{t}_1+{}^s\breve{D}^T\breve{t}_2+{}^s\breve{F}^T\breve{t}_3\right)+\left({}^s\breve{B}^C\breve{c}_1+{}^s\breve{D}^C\breve{c}_2+{}^s\breve{F}^C\breve{c}_3\right)\right]
\end{aligned}
\tag{30}
$$

in which:

$$
\begin{aligned}
&\left\{\breve{A}^T,\breve{B}^T,\breve{D}^T\right\}=\sum_{n=1}^{3}\int_{h_{n-1}}^{h_n}\frac{\breve{E}^{(n)}\left(x_3\right)}{1-\breve{v}}\breve{\alpha}^{(n)}\left(x_3\right)\left\{1,\bar{x}_3,\bar{x}_3^2\right\}dx_3,\\
&\left\{\breve{A}^C,\breve{B}^C,\breve{D}^C\right\}=\sum_{n=1}^{3}\int_{h_{n-1}}^{h_n}\frac{\breve{E}^{(n)}\left(x_3\right)}{1-\breve{v}}\breve{\beta}^{(n)}\left(x_3\right)\left\{1,\bar{x}_3,\bar{x}_3^2\right\}dx_3,\\
&\left\{a\breve{B}^T,a\breve{D}^T\right\}=\sum_{n=1}^{3}\int_{h_{n-1}}^{h_n}\frac{\breve{E}^{(n)}\left(x_3\right)}{1-\breve{v}}\breve{\alpha}^{(n)}\left(x_3\right)\bar{\breve{\Psi}}\left(x_3\right)\left\{1,\bar{x}_3\right\}dx_3,\\
&\left\{\breve{a}^c,a\breve{D}^c\right\}=\sum_{n=1}^{3}\int_{h_{n-1}}^{h_n}\frac{\breve{E}^{(n)}\left(x_3\right)}{1-\breve{v}}\breve{\beta}^{(n)}\left(x_3\right)\bar{\breve{\Psi}}\left(x_3\right)\left\{1,\bar{x}_3\right\}dx_3,\\
&\left\{s\breve{B}^T,s\breve{D}^T,s\breve{F}^T\right\}=\sum_{n=1}^{3}\int_{h_{n-1}}^{h_n}\frac{\breve{E}^{(n)}\left(x_3\right)}{1-\breve{v}}\breve{\alpha}^{(n)}\left(x_3\right)\bar{\breve{f}}\left(x_3\right)\left\{1,\bar{x}_3,\bar{\breve{\Psi}}\left(x_3\right)\right\}dx_3,\\
&\left\{s\breve{B}^c,s\breve{D}^c,s\breve{F}^c\right\}=\sum_{n=1}^{3}\int_{h_{n-1}}^{h_n}\frac{\breve{E}^{(n)}\left(x_3\right)}{1-\breve{\beta}}\breve{\beta}^{(n)}\left(x_3\right)\bar{\breve{f}}\left(x_3\right)\left\{1,\overline{x_3},\bar{\breve{\Psi}}\left(x_3\right)\right\}dx_3
\end{aligned}
\tag{31}
$$

and:

$$
\bar{x}_3=\frac{x_3}{h},\ \bar{\breve{f}}\left(x_3\right)=\frac{\breve{f}\left(x_3\right)}{h},\bar{\breve{K}}_w=\frac{\int_0^a\breve{K}_W dx}{a},\bar{\breve{\Psi}}\left(x_3\right)=\frac{1}{\pi}\sin\left(\frac{\pi x_3}{h}\right)
\tag{32}
$$

3. Results

In this part, we present and analyze several numerical examples to investigate the hygro-thermo-mechanical bending responses of FG square sandwich plates supported by elastic foundations with variable two parameters.

Comparisons are made with the proposed model. The FG square sandwich plates comprise Titanium and Zirconia, each characterized by specific material properties as follows:

Table 1: Material properties of metals and ceramics in FGM

	Ti-6Al-4V	ZrO_2
Young's modulus (GPa)	66,20	117,00
Poisson's ratio	1/3	1/3
Thermal expansion coefficient (10−6/K)	10,30	7,11
Moisture expansion coefficient	0,33	0,00

Unless specified otherwise, we assume $\breve{q}_0$ = 100 GPa, a/h = 10, $\breve{t}_1$ = 0, and $\breve{c}_1$ = 0.

Additionally, we utilize a shear correction factor of K = 5/6 in FSDT.

Numerical results are presented in terms of dimensionless stresses and deflection, with various dimensionless parameters being employed as:

center deflection:

$$\bar{X}_3 = \frac{10^2 h}{a^2 \breve{q}_0} X_3\left(\frac{a}{2},\frac{b}{2}\right), \hat{X}_3 = \frac{10^3}{\breve{q}_0 a^4 / \left(\breve{E}_0 h^3\right) + 10^3 \breve{\alpha}_0 \breve{t}_2 a^2 / h} X_3\left(\frac{a}{2},\frac{b}{2}\right)$$

axial stress:

$$\bar{\breve{\sigma}}_{x_1} = \frac{10h^2}{a^2 q_0} \breve{\sigma}_{x_1}\left(\frac{a}{2},\frac{b}{2},\frac{h}{2}\right), \hat{\breve{\sigma}}_{x_1} = \frac{10^3}{\breve{q}_0 a^2 / h^2 + 10\breve{E}_0 \breve{\alpha}_0 \breve{t}_2 a^2 / h^2} \breve{\sigma}_{x_1}\left(\frac{a}{2},\frac{b}{2},\frac{h}{2}\right)$$

transversal shear stress:

$$\bar{\breve{\tau}}_{x_1 x_3} = \frac{h}{a\breve{q}_0} \breve{\tau}_{xz}\left(0,\frac{b}{2},0\right), \hat{\breve{\tau}}_{x_1 x_3} = \frac{10^3}{\breve{q}_0 a / h + \breve{E}_0 \breve{\alpha}_0 \breve{t}_2 a / 10h} \breve{\tau}_{xz}\left(0,\frac{b}{2},0\right)$$

where $\breve{E}_0$ = 1Gpa, $\breve{\alpha}_0$ = 10-6/K.

Pasternak foundation parameter:

$$\breve{k}_w = \frac{12a^4\left(1-\breve{v}^2\right)}{h^3 \breve{E}_c} \breve{K}_w, \breve{k}_g = \frac{12a^2\left(1-\breve{v}^2\right)}{h^3 \breve{E}_c} \breve{K}_g$$

In Table 2, the calculation model is validated against documented scientific results for a FG square sandwich plates subjected to mechanical thermal loading without the elastic foundations.

Moving to Table 3, we extend this validation to another scenario involving an FG square sandwich plates under mechanical loading with the presence of the elastic foundations.

Notably, Table 3 provides a comparative analysis of results obtained from an FG square sandwich plates consisting of aluminum (Al) and zirconia (ZrO2). Young's modulus is taken for aluminum and for zirconia 70 GPa, and 151 GPa. Poisson's ratio is chosen as constant $\breve{\nu}$ = 0.3.

Table 2: Dimensionless deflections and stress of the FGM plate.

r	Theory	$\hat{X}_3$	$\hat{\hat{\sigma}}_{x_1}$	$\hat{\hat{\tau}}_{x_1x_3}$
0	present	0,796783	−2,388909	0,171603
	Ref[26]	0,808168	−2,461177	0,174481
	Ref[36]	0,895735	−3,597007	0,173624
	Ref[29]	0,895427	−2,650327	0,163882
1	present	1,011263	−2,659816	0,289195
	Ref[26]	1,025367	−2,730494	0,280495
	Ref[36]	1,132449	−3,756017	0,203004
	Ref[29]	1,136261	−2,961917	0,280083
3	present	1,092312	−2,262512	0,282953
	Ref[26]	1,107475	−2,328042	0,276238
	Ref[36]	1,223232	−3,311823	0,221768
	Ref[29]	1,227011	−2,517070	0,273899
5	present	1,112660	−2,162596	0,273950
	Ref[26]	1,128152	−2,226550	0,269077
	Ref[36]	1,246833	−3,196423	0,228818
	Ref[29]	1,249763	−2,405376	0,265250

Table 3: Dimensionless deflections $\bar{X}_3$ of the FGM plate.

		$\breve{K}_w$=0			$\breve{K}_w$=50			$\breve{K}_w$=100		
r	Theory	$\breve{K}_g$=0	$\breve{K}_g$=50	$\breve{K}_g$=100	$\breve{K}_g$=0	$\breve{K}_g$=50	$\breve{K}_g$=100	$\breve{K}_g$=0	$\breve{K}_g$=50	$\breve{K}_g$=100
0	present	0,1960	0,0533	0,0309	0,1726	0,0514	0,0302	0,1542	0,0497	0,0296
	Ref[37]	0,1961	0,0533	0,0309	0,1727	0,0514	0,0302	0,1542	0,0497	0,0296
1	present	0,2919	0,0586	0,0326	0,2429	0,0563	0,0318	0,2080	0,0542	0,0311
	Ref[37]	0,2920	0,0586	0,0326	0,2429	0,0563	0,0318	0,2080	0,0542	0,0312
2	present	0,3328	0,0601	0,0330	0,2705	0,0577	0,0323	0,2279	0,0554	0,0316
	Ref[37]	0,3329	0,0601	0,0330	0,2706	0,0577	0,0323	0,2280	0,0554	0,0316
5	present	0,3713	0,0612	0,0333	0,2954	0,0587	0,0326	0,2453	0,0564	0,0319
	Ref[37]	0,3714	0,0612	0,0333	0,2955	0,0587	0,0326	0,2454	0,0564	0,0319

Tables 2-3 show how the results of the methodology applied in this study converge with data from the literature, allowing us to expand the area of our research.

For this investigation, five FGM sandwich plates with layer thickness ratios of 1-1-1, 1-2-1, 2-1-2, 1-1-2, and 2-2-1 were chosen; three of these plates are symmetric and two are asymmetric. The analysis involved the utilization of three distinct shape functions: Reissner, Reddy, and Touratier, to compute the dimensionless center deflections ($\bar{X}_3$), normal stress ($\bar{\bar{\sigma}}_{x_1}$), and transverse shear stress ($\bar{\bar{\tau}}_{x_1x_3}$) across various volume fraction indices (r = 0, 1, 3, 5).

These calculations were conducted both with and without the presence of an elastic foundation.

The resultant findings are presented in Tables 4–8, respectively.

Table 4. Dimensionless deflections and stress of the FGM plate with layer thickness ratios1-1-1.

r	$\breve{K}_w$	$\breve{K}_g$	Theory	$\breve{t}_2 = \breve{t}_3 = 10, \breve{c}_2 = \breve{c}_3 = 100$			$\breve{t}_3 = \breve{c}_3 = 0, \breve{t}_2 = 10, \breve{c}_2 = 100$		
				$\bar{X}_3$	$\bar{\bar{\sigma}}_{x_1}$	$\bar{\bar{\tau}}_{x_1x_3}$	$\bar{X}_3$	$\bar{\bar{\sigma}}_{x_1}$	$\bar{\bar{\tau}}_{x_1x_3}$
0	0	0	Touratier	1,09949	-0,78489	2,40429	0,72807	-0,03200	2,46170
			Reddy	1,11203	-0,86553	2,33901	0,72809	-0,03327	2,38564
			Reissner	1,20802	-1,07359	2,32735	0,72809	-0,03327	2,38564
		100	Touratier	0,17273	-8,44289	-6,80208	0,11438	-5,10304	-3,63466
			Reddy	0,17469	-8,60551	-6,68403	0,11437	-5,10094	-3,52210
			Reissner	0,18977	-9,48165	-7,47451	0,11437	-5,10094	-3,52210
	100	0	Touratier	0,86450	-2,72661	0,06998	0,57247	-1,31778	0,91594
			Reddy	0,87435	-2,82814	0,05105	0,57247	-1,31827	0,88763
			Reissner	0,94982	-3,20561	-0,15809	0,57247	-1,31827	0,88763
		100	Touratier	0,16566	-8,50134	-6,87235	0,10970	-5,14175	-3,68120
			Reddy	0,16753	-8,66458	-6,75289	0,10969	-5,13962	-3,56719
			Reissner	0,18199	-9,54582	-7,54932	0,10969	-5,13962	-3,56719
1	0	0	Touratier	1,64281	-3,06408	2,79154	1,07376	-1,55314	2,75852
			Reddy	1,66204	-3,17374	2,70700	1,07374	-1,55410	2,67198
			Reissner	1,80911	-3,57865	2,71576	1,35425	-0,17550	2,50212
		100	Touratier	0,19796	-9,88889	-8,48970	0,12939	-6,01390	-4,61501
			Reddy	0,20025	-10,07364	-8,39998	0,12937	-6,01171	-4,50359
			Reissner	0,21797	-11,08912	-9,37408	0,16317	-5,79765	-6,54802
	100	0	Touratier	1,19936	-5,15877	-0,67093	0,78391	-2,92225	0,49541
			Reddy	1,21333	-5,29171	-0,70236	0,78386	-2,92239	0,46939
			Reissner	1,32070	-5,88404	-0,99529	0,98864	-1,90126	-0,27587
		100	Touratier	0,18952	-9,92878	-8,55563	0,12387	-6,03997	-4,65811
			Reddy	0,19171	-10,11395	-8,46488	0,12385	-6,03776	-4,54552
			Reissner	0,20867	-11,13300	-9,44472	0,15621	-5,83050	-6,60090
2	0	0	Touratier	1,79661	-2,31175	2,85067	1,17447	-1,06116	2,82595
			Reddy	1,81755	-2,41324	2,77254	1,17450	-1,06212	2,74552
			Reissner	1,97831	-2,75103	2,77929	1,35135	-0,19179	2,58778
		100	Touratier	0,19913	-9,87563	-8,82331	0,13017	-6,00576	-4,80547
			Reddy	0,20140	-10,05964	-8,75313	0,13014	-6,00321	-4,70236
			Reissner	0,21921	-11,07374	-9,76583	0,14974	-5,87687	-5,98153
	100	0	Touratier	1,27744	-4,76997	-0,94332	0,83508	-2,66813	0,34578
			Reddy	1,29222	-4,89870	-0,97388	0,83503	-2,66822	0,32459
			Reissner	1,40652	-5,45632	-1,29849	0,96076	-2,03972	-0,19767
		100	Touratier	0,19055	-9,91627	-8,88604	0,12456	-6,03233	-4,84647
			Reddy	0,19272	-10,10071	-8,81504	0,12453	-6,02975	-4,74237
			Reissner	0,20976	-11,11845	-9,83321	0,14329	-5,90741	-6,02756
5	0	0	Touratier	1,92182	-1,69927	2,89801	1,25787	-0,65414	2,89917
			Reddy	1,94423	-1,79394	2,83353	1,25798	-0,65503	2,83013
			Reissner	2,11579	-2,07867	2,83438	1,35162	-0,19341	2,71279
		100	Touratier	0,19896	-9,86771	-9,20894	0,13023	-6,00053	-5,02504
			Reddy	0,20120	-10,05086	-9,16383	0,13019	-5,99755	-4,93260
			Reissner	0,21896	-11,06418	-10,22164	0,13988	-5,93359	-5,62773
	100	0	Touratier	1,33583	-4,47760	-1,21993	0,87432	-2,47261	0,20391
			Reddy	1,35122	-4,60310	-1,24819	0,87429	-2,47265	0,18911
			Reissner	1,47045	-5,13571	-1,60752	0,93936	-2,14632	-0,12480
		100	Touratier	0,19032	-9,90869	-9,26968	0,12457	-6,02735	-5,06480
			Reddy	0,19246	-10,09226	-9,22400	0,12453	-6,02434	-4,97153
			Reissner	0,20945	-11,10925	-10,28712	0,13380	-5,96237	-5,66956

Table 5. Dimensionless deflections and stress of the FGM plate with layer thickness ratios1-2-1.

r	$\breve{K}_w$	$\breve{K}_g$	Theory	$\breve{t}_2=\breve{t}_3=10, \breve{c}_2=\breve{c}_3=100$			$\breve{t}_3=\breve{c}_3=0, \breve{t}_2=10, \breve{c}_2=100$		
				$\bar{X}_3$	$\bar{\bar{\sigma}}_{x_1}$	$\bar{\bar{\tau}}_{x_1x_3}$	$\bar{X}_3$	$\bar{\bar{\sigma}}_{x_1}$	$\bar{\bar{\tau}}_{x_1x_3}$
0	0	0	Touratier	1,09949	-0,78489	2,40429	0,72807	-0,03200	2,46170
			Reddy	1,11203	-0,86553	2,33901	0,72809	-0,03327	2,38564
			Reissner	1,20802	-1,07359	2,32735	0,72809	-0,03327	2,38564
		100	Touratier	0,17273	-8,44289	-6,80208	0,11438	-5,10304	-3,63466
			Reddy	0,17469	-8,60551	-6,68403	0,11437	-5,10094	-3,52210
			Reissner	0,18977	-9,48165	-7,47451	0,11437	-5,10094	-3,52210
	100	0	Touratier	0,86450	-2,72661	0,06998	0,57247	-1,31778	0,91594
			Reddy	0,87435	-2,82814	0,05105	0,57247	-1,31827	0,88763
			Reissner	0,94982	-3,20561	-0,15809	0,57247	-1,31827	0,88763
		100	Touratier	0,16566	-8,50134	-6,87235	0,10970	-5,14175	-3,68120
			Reddy	0,16753	-8,66458	-6,75289	0,10969	-5,13962	-3,56719
			Reissner	0,18199	-9,54582	-7,54932	0,10969	-5,13962	-3,56719
1	0	0	Touratier	1,53704	-3,58181	2,76487	1,00682	-1,88015	2,71457
			Reddy	1,55502	-3,69736	2,67245	1,00676	-1,88115	2,62171
			Reissner	1,69208	-4,15141	2,68513	1,00676	-1,88115	2,62171
		100	Touratier	0,19446	-9,91598	-8,05182	0,12738	-6,02929	-4,37080
			Reddy	0,19672	-10,10152	-7,95303	0,12736	-6,02738	-4,25752
			Reissner	0,21406	-11,12006	-8,87690	0,12736	-6,02738	-4,25752
	100	0	Touratier	1,13874	-5,46094	-0,44407	0,74592	-3,11106	0,61258
			Reddy	1,15204	-5,59734	-0,47990	0,74586	-3,11125	0,58079
			Reissner	1,25358	-6,21886	-0,74508	0,74586	-3,11125	0,58079
		100	Touratier	0,18622	-9,95486	-8,11821	0,12198	-6,05476	-4,41429
			Reddy	0,18838	-10,14083	-8,01824	0,12197	-6,05283	-4,29974
			Reissner	0,20499	-11,16283	-8,94786	0,12197	-6,05283	-4,29974
2	0	0	Touratier	1,66435	-2,95919	2,82083	1,08997	-1,47384	2,76392
			Reddy	1,68374	-3,06790	2,72837	1,08991	-1,47488	2,67232
			Reissner	1,83220	-3,46615	2,74239	1,08991	-1,47488	2,67232
		100	Touratier	0,19600	-9,90388	-8,25250	0,12836	-6,02184	-4,48787
			Reddy	0,19826	-10,08891	-8,16660	0,12834	-6,01969	-4,38018
			Reissner	0,21574	-11,10621	-9,11321	0,12834	-6,01969	-4,38018
	100	0	Touratier	1,20647	-5,12480	-0,63225	0,79010	-2,89208	0,50254
			Reddy	1,22048	-5,25747	-0,66933	0,79004	-2,89222	0,47293
			Reissner	1,32809	-5,84878	-0,95490	0,79004	-2,89222	-2,89222
		100	Touratier	0,18762	-9,94354	-8,31573	0,12287	-6,04781	-4,52928
			Reddy	0,18978	-10,12900	-8,22882	0,12285	-6,04564	-4,42045
			Reissner	0,20651	-11,14983	-9,18091	0,12285	-6,04564	-4,42045
5	0	0	Touratier	1,77771	-2,40440	2,85019	1,16503	-1,10687	-1,10687
			Reddy	1,79837	-2,50703	2,76384	1,16501	-1,10790	2,71562
			Reissner	1,95671	-2,85681	2,77590	1,16501	-1,10790	2,71562
		100	Touratier	0,19635	-9,89797	-8,43889	0,12868	-6,01781	-4,59691
			Reddy	0,19859	-10,08245	-8,37139	0,12865	-6,01538	-4,49796
			Reissner	0,21608	-11,09921	-9,33975	0,12865	-6,01538	-4,49796
	100	0	Touratier	1,26256	-4,84551	-0,82735	0,82742	-2,70667	0,39134
			Reddy	1,27716	-4,97512	-0,86405	0,82736	-2,70677	0,36541
			Reissner	1,38961	-5,54221	-1,17142	0,82736	-2,70677	0,36541
		100	Touratier	0,18788	-9,93809	-8,49933	0,12313	-6,04411	-4,63652
			Reddy	0,19003	-10,12300	-8,43100	0,12310	-6,04165	-4,53658
			Reissner	0,20676	-11,14334	-9,40460	0,12310	-6,04165	-4,53658

Table 6. Dimensionless deflections and stress of the FGM plate with layer thickness ratios2-1-2.

r	$\breve{K}_w$	$\breve{K}_g$	Theory	$\breve{t}_2=\breve{t}_3=10, \breve{c}_2=\breve{c}_3=100$			$\breve{t}_3=\breve{c}_3=0, \breve{t}_2=10, \breve{c}_2=100$		
				$\bar{X}_3$	$\bar{\bar{\sigma}}_{x_1}$	$\bar{\bar{\tau}}_{x_1x_3}$	$\bar{X}_3$	$\bar{\bar{\sigma}}_{x_1}$	$\bar{\bar{\tau}}_{x_1x_3}$
0	0	0	Touratier	1,09949	-0,78489	2,40429	0,72807	-0,03200	2,46170
			Reddy	1,11203	-0,86553	2,33901	0,72809	-0,03327	2,38564
			Reissner	1,20802	-1,07359	2,32735	0,72809	-0,03327	2,38564
		100	Touratier	0,17273	-8,44289	-6,80208	0,11438	-5,10304	-3,63466
			Reddy	0,17469	-8,60551	-6,68403	0,11437	-5,10094	-3,52210
			Reissner	0,18977	-9,48165	-7,47451	0,11437	-5,10094	-3,52210
	100	0	Touratier	0,86450	-2,72661	0,06998	0,57247	-1,31778	0,91594
			Reddy	0,87435	-2,82814	0,05105	0,57247	-1,31827	0,88763
			Reissner	0,94982	-3,20561	-0,15809	0,57247	-1,31827	0,88763
		100	Touratier	0,16566	-8,50134	-6,87235	0,10970	-5,14175	-3,68120
			Reddy	0,16753	-8,66458	-6,75289	0,10969	-5,13962	-3,56719
			Reissner	0,18199	-9,54582	-7,54932	0,10969	-5,13962	-3,56719
1	0	0	Touratier	1,70908	-2,74030	2,83259	1,11591	-1,34786	2,81607
			Reddy	1,72906	-2,84641	2,75372	1,11594	-1,34880	2,73333
			Reissner	1,88234	-3,22081	2,75882	1,11594	-1,34880	2,73333
		100	Touratier	0,19968	-9,87185	-8,87094	0,13038	-6,00430	-4,82557
			Reddy	0,20197	-10,05610	-8,78373	0,13035	-6,00194	-4,71294
			Reissner	0,21988	-11,06965	-9,80143	0,13035	-6,00194	-4,71294
	100	0	Touratier	1,23582	-4,97632	-0,83692	0,80691	-2,80784	0,42012
			Reddy	1,25019	-5,10726	-0,86425	0,80687	-2,80796	0,39830
			Reissner	1,36102	-5,68209	-1,17988	0,80687	-2,80796	0,39830
		100	Touratier	0,19113	-9,91226	-8,93725	0,12479	-6,03068	-4,86886
			Reddy	0,19332	-10,09694	-8,84908	0,12477	-6,02829	-4,75511
			Reissner	0,21046	-11,11410	-9,87257	0,12477	-6,02829	-4,75511
2	0	0	Touratier	1,87307	-1,93863	2,91790	1,22376	-0,82175	2,92045
			Reddy	1,89489	-2,03607	2,84889	1,22385	-0,82266	2,84598
			Reissner	2,06265	-2,33942	2,84962	1,22385	-0,82266	2,84598
		100	Touratier	0,20032	-9,85758	-9,36306	0,13088	-5,99557	-5,10326
			Reddy	0,20259	-10,04094	-9,29691	0,13084	-5,99276	-4,99863
			Reissner	0,22052	-11,05298	-10,37149	0,13084	-5,99276	-4,99863
	100	0	Touratier	1,31625	-4,57467	-1,17016	0,85996	-2,54400	0,24954
			Reddy	1,33143	-4,70131	-1,19508	0,85993	-2,54406	0,23410
			Reissner	1,44931	-5,24062	-1,55237	0,85993	-2,54406	0,23410
		100	Touratier	0,19165	-9,89863	-9,42672	0,12521	-6,02238	-5,14485
			Reddy	0,19382	-10,08242	-9,35985	0,12518	-6,01955	-5,03928
			Reissner	0,21098	-11,09813	-10,43999	0,12518	-6,01955	-5,03928
5	0	0	Touratier	1,99294	-1,35377	3,02907	1,30428	-0,43050	3,06756
			Reddy	2,01620	-1,44459	2,97516	1,30448	-0,43133	3,00455
			Reissner	2,19414	-1,69790	2,96781	1,30448	-0,43133	3,00455
		100	Touratier	0,19962	-9,84622	-10,01711	0,13064	-5,98841	-5,47055
			Reddy	0,20185	-10,02853	-9,97244	0,13060	-5,98511	-5,37251
			Reissner	0,21966	-11,03939	-11,12242	0,13060	-5,98511	-5,37251
	100	0	Touratier	1,36960	-4,30564	-1,50562	0,89634	-2,36236	0,09982
			Reddy	1,38535	-4,42922	-1,52672	0,89632	-2,36238	0,09185
			Reissner	1,50761	-4,94593	-1,93136	0,89632	-2,36238	0,09185
		100	Touratier	0,19092	-9,88743	-10,08042	0,12494	-6,01539	-5,51199
			Reddy	0,19305	-10,07017	-10,03525	0,12490	-6,01205	-5,41314
			Reissner	0,21008	-11,08470	-11,19077	0,12490	-6,01205	-5,41314

Table 7. Dimensionless deflections and stress of the FGM plate with layer thickness ratios1-1-2.

r	$\breve{K}_w$	$\breve{K}_g$	Theory	$\breve{t}_2 = \breve{t}_3 = 10, \breve{c}_2 = \breve{c}_3 = 100$			$\breve{t}_3 = \breve{c}_3 = 0, \breve{t}_2 = 10, \breve{c}_2 = 100$		
				$\bar{X}_3$	$\bar{\bar{\sigma}}_{x_1}$	$\bar{\bar{\tau}}_{x_1x_3}$	$\bar{X}_3$	$\bar{\bar{\sigma}}_{x_1}$	$\bar{\bar{\tau}}_{x_1x_3}$
0	0	0	Touratier	1,09949	-0,78489	2,40429	0,72807	-0,03200	2,46170
			Reddy	1,11203	-0,86553	2,33901	0,72809	-0,03327	2,38564
			Reissner	1,20802	-1,07359	2,32735	0,72809	-0,03327	2,38564
		100	Touratier	0,17273	-8,44289	-6,80208	0,11438	-5,10304	-3,63466
			Reddy	0,17469	-8,60551	-6,68403	0,11437	-5,10094	-3,52210
			Reissner	0,18977	-9,48165	-7,47451	0,11437	-5,10094	-3,52210
	100	0	Touratier	0,86450	-2,72661	0,06998	0,57247	-1,31778	0,91594
			Reddy	0,87435	-2,82814	0,05105	0,57247	-1,31827	0,88763
			Reissner	0,94982	-3,20561	-0,15809	0,57247	-1,31827	0,88763
		100	Touratier	0,16566	-8,50134	-6,87235	0,10970	-5,14175	-3,68120
			Reddy	0,16753	-8,66458	-6,75289	0,10969	-5,13962	-3,56719
			Reissner	0,18199	-9,54582	-7,54932	0,10969	-5,13962	-3,56719
1	0	0	Touratier	1,65821	-3,30141	2,85235	1,08395	-1,70025	2,82836
			Reddy	1,67758	-3,41378	2,76734	1,08394	-1,70124	2,73995
			Reissner	1,82599	-3,84192	2,77419	1,08394	-1,70124	2,73995
		100	Touratier	0,19789	-9,97403	-8,75978	0,12936	-6,06204	-4,76231
			Reddy	0,20017	-10,15948	-8,66035	0,12934	-6,05985	-4,64384
			Reissner	0,21788	-11,18438	-9,66448	0,12934	-6,05985	-4,64384
	100	0	Touratier	1,20698	-5,36320	-0,73572	0,78898	-3,04801	0,48290
			Reddy	1,22102	-5,49837	-0,76411	0,78894	-3,04816	0,45817
			Reissner	1,32904	-6,11093	-1,06968	0,78894	-3,04816	0,45817
		100	Touratier	0,18944	-10,01264	-8,82698	0,12383	-6,08728	-4,80624
			Reddy	0,19162	-10,19851	-8,72648	0,12381	-6,08507	-4,68656
			Reissner	0,20857	-11,22687	-9,73646	0,12381	-6,08507	-4,68656
2	0	0	Touratier	1,80584	-2,66432	2,96183	1,18116	-1,28194	2,94747
			Reddy	1,82685	-2,76972	2,88048	1,18119	-1,28297	2,86203
			Reissner	1,98827	-3,14141	-3,14141	1,18119	-1,28297	2,86203
		100	Touratier	0,19856	-9,96130	-9,23841	0,12987	-6,05474	-5,03243
			Reddy	0,20083	-10,14594	-9,14999	0,12985	-6,05221	-4,91651
			Reissner	0,21857	-11,16937	-10,20836	0,12985	-6,05221	-4,91651
	100	0	Touratier	1,28067	-5,04858	-1,02456	0,83766	-2,84144	0,34007
			Reddy	1,29548	-5,18023	-1,05102	0,83762	-2,84153	0,32004
			Reissner	1,40994	-5,76491	-1,39379	0,83762	-2,84153	0,32004
		100	Touratier	0,18999	-10,00020	-9,30344	0,12427	-6,08018	-5,07497
			Reddy	0,19216	-10,18524	-9,21409	0,12425	-6,07762	-4,95796
			Reissner	0,20914	-11,21215	-10,27813	0,12425	-6,07762	-4,95796
5	0	0	Touratier	1,91507	-2,17969	3,10546	1,25451	-0,95893	3,11312
			Reddy	1,93737	-2,27974	3,02901	1,25459	-0,95998	3,03036
			Reissner	2,10806	-2,60968	3,02867	1,25459	-0,95998	3,03036
		100	Touratier	0,19801	-9,94589	-9,86700	0,12971	-6,04634	-5,38476
			Reddy	0,20026	-10,12979	-9,78373	0,12968	-6,04347	-5,26684
			Reissner	0,21790	-11,15137	-10,91295	0,12968	-6,04347	-5,26684
	100	0	Touratier	1,33056	-4,82343	-1,31058	0,87161	-2,69077	0,22030
			Reddy	1,34591	-4,95256	-1,33353	0,87158	-2,69083	0,20529
			Reissner	1,46449	-5,51799	-1,71823	0,87158	-2,69083	0,20529
		100	Touratier	0,18941	-9,98481	-9,93200	0,12408	-6,07184	-5,42734
			Reddy	0,19156	-10,16911	-9,84791	0,12405	-6,06893	-5,30840
			Reissner	0,20843	-11,19415	-10,98278	0,12405	-6,06893	-5,30840

Table 8. Dimensionless deflections and stress of the FGM plate with layer thickness ratios2-2-1.

r	$\breve{K}_w$	$\breve{K}_g$	Theory	$\breve{t}_2 = \breve{t}_3 = 10, \breve{c}_2 = \breve{c}_3 = 100$			$\breve{t}_3 = \breve{c}_3 = 0, \breve{t}_2 = 10, \breve{c}_2 = 100$		
				$\bar{X}_3$	$\bar{\bar{\sigma}}_{x_1}$	$\bar{\bar{\tau}}_{x_1x_3}$	$\bar{X}_3$	$\bar{\bar{\sigma}}_{x_1}$	$\bar{\bar{\tau}}_{x_1x_3}$
0	0	0	Touratier	1,09949	-0,78489	2,40429	0,72807	-0,03200	2,46170
			Reddy	1,11203	-0,86553	2,33901	0,72809	-0,03327	2,38564
			Reissner	1,20802	-1,07359	2,32735	0,72809	-0,03327	2,38564
		100	Touratier	0,17273	-8,44289	-6,80208	0,11438	-5,10304	-3,63466
			Reddy	0,17469	-8,60551	-6,68403	0,11437	-5,10094	-3,52210
			Reissner	0,18977	-9,48165	-7,47451	0,11437	-5,10094	-3,52210
	100	0	Touratier	0,86450	-2,72661	0,06998	0,57247	-1,31778	0,91594
			Reddy	0,87435	-2,82814	0,05105	0,57247	-1,31827	0,88763
			Reissner	0,94982	-3,20561	-0,15809	0,57247	-1,31827	0,88763
		100	Touratier	0,16566	-8,50134	-6,87235	0,10970	-5,14175	-3,68120
			Reddy	0,16753	-8,66458	-6,75289	0,10969	-5,13962	-3,56719
			Reissner	0,18199	-9,54582	-7,54932	0,10969	-5,13962	-3,56719
1	0	0	Touratier	1,58316	-3,07372	2,78777	1,03611	-1,56020	2,75208
			Reddy	1,60165	-3,18369	2,70058	1,03608	-1,56116	2,66269
			Reissner	1,74305	-3,58932	2,71005	1,03608	-1,56116	2,66269
		100	Touratier	0,19578	-9,81439	-8,32931	0,12813	-5,97168	-4,52356
			Reddy	0,19805	-9,99870	-8,23125	0,12811	-5,96965	-4,40886
			Reissner	0,21553	-11,00597	-9,18685	0,12811	-5,96965	-4,40886
	100	0	Touratier	1,16495	-5,10562	-0,56335	0,76241	-2,88999	0,55892
			Reddy	1,17852	-5,23816	-0,59496	0,76236	-2,89015	0,53088
			Reissner	1,28256	-5,82516	-0,87642	0,76236	-2,89015	0,53088
		100	Touratier	0,18746	-9,85483	-8,39600	0,12269	-5,99814	-5,99814
			Reddy	0,18963	-10,03958	-8,29682	0,12267	-5,99609	-4,45128
			Reissner	0,20637	-11,05045	-9,25820	0,12267	-5,99609	-4,45128
2	0	0	Touratier	1,71788	-2,32858	2,85904	1,12441	-1,07272	2,82462
			Reddy	1,73788	-2,43046	2,77443	1,12441	-1,07368	2,73803
			Reissner	1,89125	-2,76966	2,78354	1,12441	-1,07368	2,73803
		100	Touratier	0,19697	-9,79508	-9,79508	0,12892	-5,95978	-4,69725
			Reddy	0,19922	-9,97885	-8,54778	0,12890	-5,95748	-4,58743
			Reissner	0,21680	-10,98419	-9,53787	0,12890	-5,95748	-4,58743
	100	0	Touratier	1,23483	-4,69998	-0,79087	0,80824	-2,62487	0,43563
			Reddy	1,24914	-4,82816	-4,82816	0,80819	-2,62499	0,41114
			Reissner	1,35937	-5,37895	-1,13028	0,80819	-2,62499	0,41114
		100	Touratier	0,18851	-9,83658	-8,69681	0,12339	-5,98695	-4,73906
			Reddy	0,19067	-10,02081	-8,61071	0,12336	-5,98463	-4,62815
			Reissner	0,20750	-11,02985	-9,60635	0,12336	-5,98463	-4,62815
5	0	0	Touratier	1,82875	-1,71653	2,92589	1,19827	-0,66579	2,90570
			Reddy	1,85004	-1,81152	2,84826	1,19832	-0,66670	2,82522
			Reissner	2,01297	-2,09773	2,85402	1,19832	-0,66670	2,82522
		100	Touratier	0,19693	-9,78557	-8,97819	0,12904	-5,95293	-4,89429
			Reddy	0,19917	-9,96877	-8,90769	0,12901	-5,95036	-4,78939
			Reissner	0,21671	-10,97338	-9,93726	0,12901	-5,95036	-4,78939
	100	0	Touratier	1,28805	-4,39020	-1,01853	0,84398	-2,41768	0,32117
			Reddy	1,30293	-4,51491	-1,04777	0,84394	-2,41775	0,30167
			Reissner	1,41767	-5,03920	-1,38513	0,84394	-2,41775	0,30167
		100	Touratier	0,18841	-9,82769	-9,04032	0,12346	-5,98053	-4,93501
			Reddy	0,19056	-10,01134	-8,96903	0,12343	-5,97793	-4,82913
			Reissner	0,20734	-11,01969	-10,00401	0,12343	-5,97793	-4,82913

It can be seen from tables 4-8 that the results obtained from the method of Reissner, Reddy, and Touratier are convergent after stabilizing the values of temperatures and moistures and changing the values of the Winkler parameter, shear layer foundation stiffness, volume fraction indices, and layer thickness ratios. If we check in all cases, we are unable to determine the method we give small or large values for the dimensionless deflection and stress.

Figure 2 shows the variation of $\bar{X}_3$ with a/h for 1-1-1 FGM sandwich plate for different values of Winkler parameter, Figure 3 shows the variation of $\bar{X}_3$ with a/h for 1-1-1 FGM sandwich plate for different values of shear layer foundation stiffness, Figure 4 shows the variation of $\bar{X}_3$ with a/h for 1-1-1 FGM sandwich under different values of temperatures, Figure 5 shows the variation of $\bar{X}_3$ with a/h for 1-1-1 FGM sandwich under different values of moistures and Figure 6 shows the variation of $\bar{X}_3$ with a/h for 1-1-1 FGM sandwich under different values of volume fraction indices r.

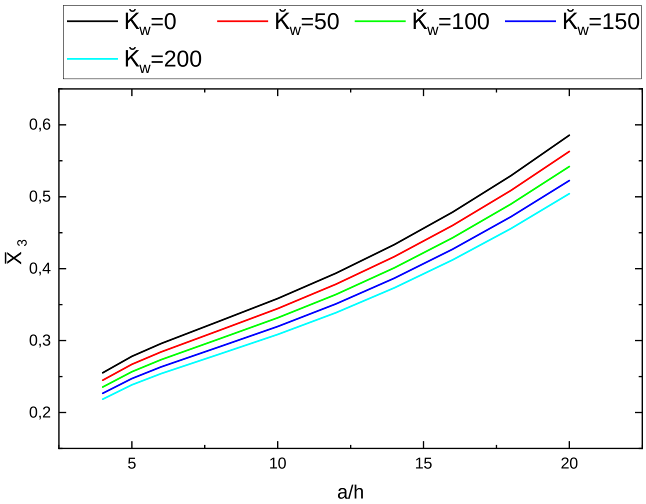

Fig 2: Variation of dimensionless deflection $\bar{X}_3$ with a/h for 1-1-1 FGM sandwich plate under different Winkler parameter.($\breve{t}_2 = \breve{t}_3 = 10, \breve{c}_2 = \breve{c}_3 = 100, \breve{t}_1 = \breve{c}_1 = 0, \breve{K}_G = 50, r = 2$)

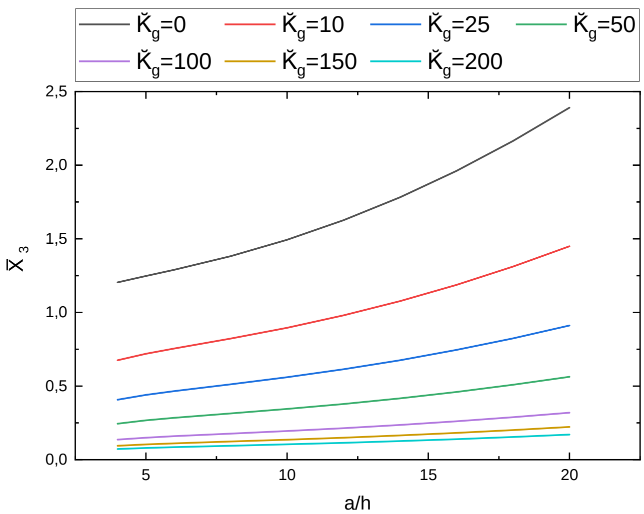

Fig 3. Variation of dimensionless deflection $\bar{X}_3$with a/h for 1-1-1 FGM sandwich plate under different shear layer foundation stiffness. ($\breve{t}_2 = \breve{t}_3 = 10, \breve{c}_2 = \breve{c}_3 = 100, \breve{t}_1 = \breve{c}_1 = 0, \breve{K}_w = 50, r = 2$)

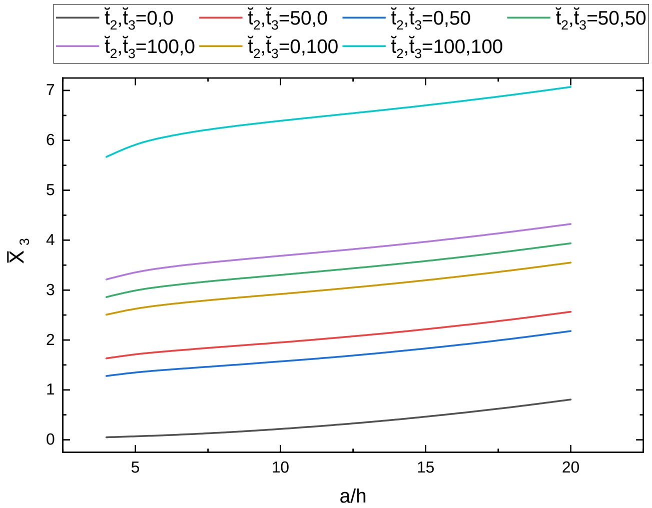

Fig 4: Variation of dimensionless deflection $\bar{X}_3$ with a/h for 1-1-1 FGM sandwich plate for different values of temperatures. ($\breve{c}_2 = \breve{c}_3 = 10, \breve{t}_1 = \breve{c}_1 = 0, \breve{K}_w = \breve{K}_G = 10, r = 2$)

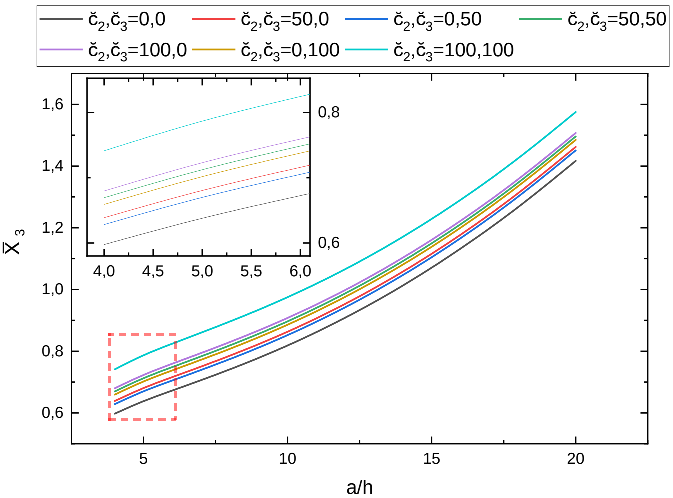

Fig 5. Variation of dimensionless deflection $\bar{X}_3$ with a/h for 1-1-1 FGM sandwich plate for different values of moistures. ($\breve{t}_2 = \breve{t}_3 = 10, \breve{t}_1 = \breve{c}_1 = 0, \breve{K}_w = \breve{K}_G = 10, r = 2$)

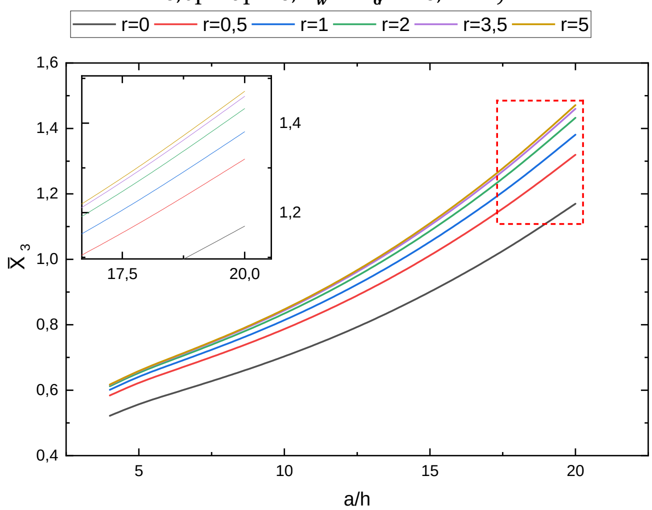

Fig 6: Variation of dimensionless deflection $\bar{X}_3$with a/h for 1-1-1 FGM sandwich plate for different volume fraction indices s. ($\breve{c}_2 = \breve{c}_3 = \breve{t}_2 = \breve{t}_3 = 10, \breve{t}_1 = \breve{c}_1 = 0, \breve{K}_w = \breve{K}_G = 10$)

Figure 2-6 demonstrates that for hygro-thermo-mechanical load, parameters foundation elastic, volume fraction indices, and layer thickness ratios, are fixed, the value of dimensionless deflection $\bar{X}_3$ increases as the plate thickness decreases. This is normal, a lack of thickness causes increased flexibility.

Figure 2 illustrates this logical relationship between an increase in the Winkler parameter values and a decrease in the dimensionless deflection $\bar{X}_3$ value. An increase in the bending resistance, one of the foundation constants that applies to the whole plate under study, is indicated by an increase in the Winkler parameter values. the same observation about the impact of shear layer foundation stiffness on the dimensionless deflection $\bar{X}_3$ value is shown in Figure 3.

It can be seen from figure 4 and 5 that an increase in hygro-thermal load, has led to increases in the value of the dimensionless deflection $\bar{X}_3$.

It can be seen from Figure 6 that when the volume fraction indices s equals zero, the dimensionless deflection $\bar{X}_3$at its minimum. A rise in this index r will cause this deflection $\bar{X}_3$ to grow. This is thus because layers of a functionally graded material are represented by the index r, which formalizes the composition between the metal and ceramic. If s is equal to zero, the plate is made entirely of ceramic, and ceramic has a higher Young's modulus than metal. Consequently, it makes sense that in this instance, the deflection $\bar{X}_3$ is less and grows as the volume fraction index r, or the proportion of metal whose Young's modulus is less than Young's modulus of ceramic, and this can be illustrated by presenting Figure 7 which shows the variation of Young's modulus E through-the-thickness x_3 of 1-1-1 FGM sandwich plate.

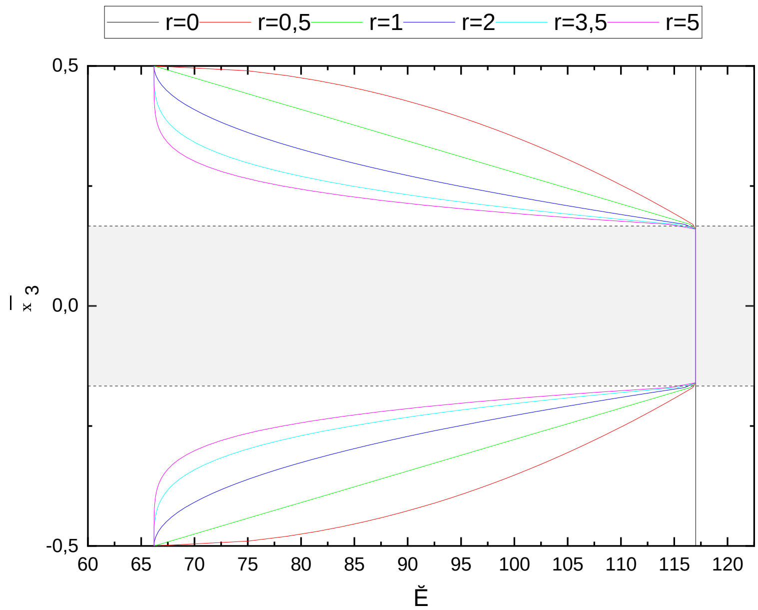

Fig 7: Variation of Young's modulus $\breve{E}$ of FGM sandwich plate 1-1-1 through-the-thickness $\bar{x}_3$

It can be seen from Figure 7 that the Young's modulus E of a plate keeps a constant value even with a change in thickness depth $\bar{x}_3$, demonstrating that the plate is entirely ceramic in this case.

When the volume fraction indices s is not equal to zero, the Young's modulus E varies as the thickness depth $\bar{x}_3$ in layers of functionally graded materials changes and it decreases as the volume fraction indices r grow, confirming the findings in Figure 6, An increase or decrease in the Young's modulus E corresponds to a respective increase or decrease in rigidity.

when the volume fraction indices r equal one the curve in the functionally graded material interval becomes straight, this is due to the simple reason that the volume fractions of metal expression $\breve{V}_m^{(1,3)}(x_3)$ in the current situation is a linear function with respect to $\bar{x}_3$.

Figure 8 shows the variation of $\bar{\bar{\sigma}}_{x_1}$ and $\bar{\bar{\tau}}_{x_1x_3}$ through-the-thickness $\bar{x}_3$ of 1-0-1 and 1-4-2 FGM sandwich plate for different values of Winkler parameter, Figure 9 shows the variation of $\bar{\bar{\sigma}}_{x_1}$ and $\bar{\bar{\tau}}_{x_1x_3}$ through-the-thickness $\bar{x}_3$ of 1-0-1 and 1-4-2 FGM sandwich plate for different values of shear layer foundation stiffness, Figure 10 shows the variation of $\bar{\bar{\sigma}}_{x_1}$ and $\bar{\bar{\tau}}_{x_1x_3}$ through-the-thickness $\bar{x}_3$ of 1-0-1 and 1-4-2 FGM sandwich plate under different values of temperatures, Figure 11 shows the variation of $\bar{\bar{\sigma}}_{x_1}$ and $\bar{\bar{\tau}}_{x_1x_3}$ through-the-thickness $\bar{x}_3$ of 1-0-1 and 1-4-2 FGM sandwich plate under different values of moistures and Figure 12 shows the variation of $\bar{\bar{\sigma}}_{x_1}$ and $\bar{\bar{\tau}}_{x_1x_3}$ through-the-thickness $\bar{x}_3$ of 1-0-1 and 1-4-2 FGM sandwich plate under different values of volume fraction indices r.

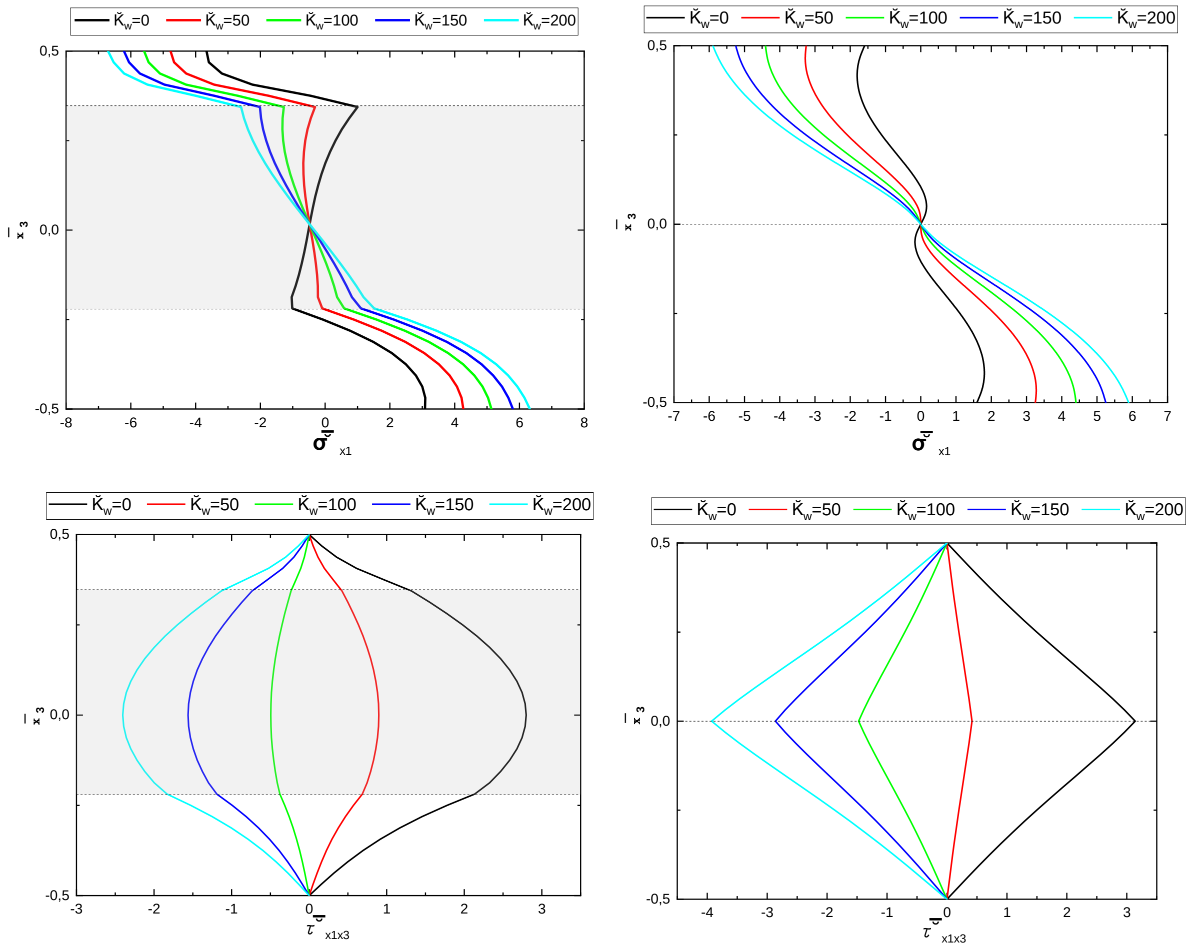

1-4-2 **1-0-1**

Fig 8: Variation of dimensionless stress $\bar{\bar{\sigma}}_{x_1}$ and $\bar{\bar{\tau}}_{x_1x_3}$ with $\bar{x}_3$ for two types of FGM sandwich plate under different value of Winkler parameter($\breve{t}_2 = \breve{t}_3 = 10, \breve{c}_2 = \breve{c}_3 = 100, \breve{t}_1 = \breve{c}_1 = 0, \breve{K}_G = 0, r = 2$)

It can be seen from Figure 8-12 that along the thickness $\bar{x}_3$ of the FGM sandwich plate, the dimensionless stresses $\bar{\bar{\sigma}}_{x_1}$ and $\bar{\bar{\tau}}_{x_1x_3}$vary continuously. The layer thickness ratios of the plate determine the distribution of various stress levels, and at each layer boundary, inflection points are observable at the level of the curves. Additionally, by Case of the Situation of the Examined Plate, these distributions may be symmetric or asymmetric. A symmetric FGM sandwich plate without a ceramic central core is represented by the case 1-0-1, whereas an asymmetric FGM sandwich plate with a ceramic central core is represented by the case 1-4-2.

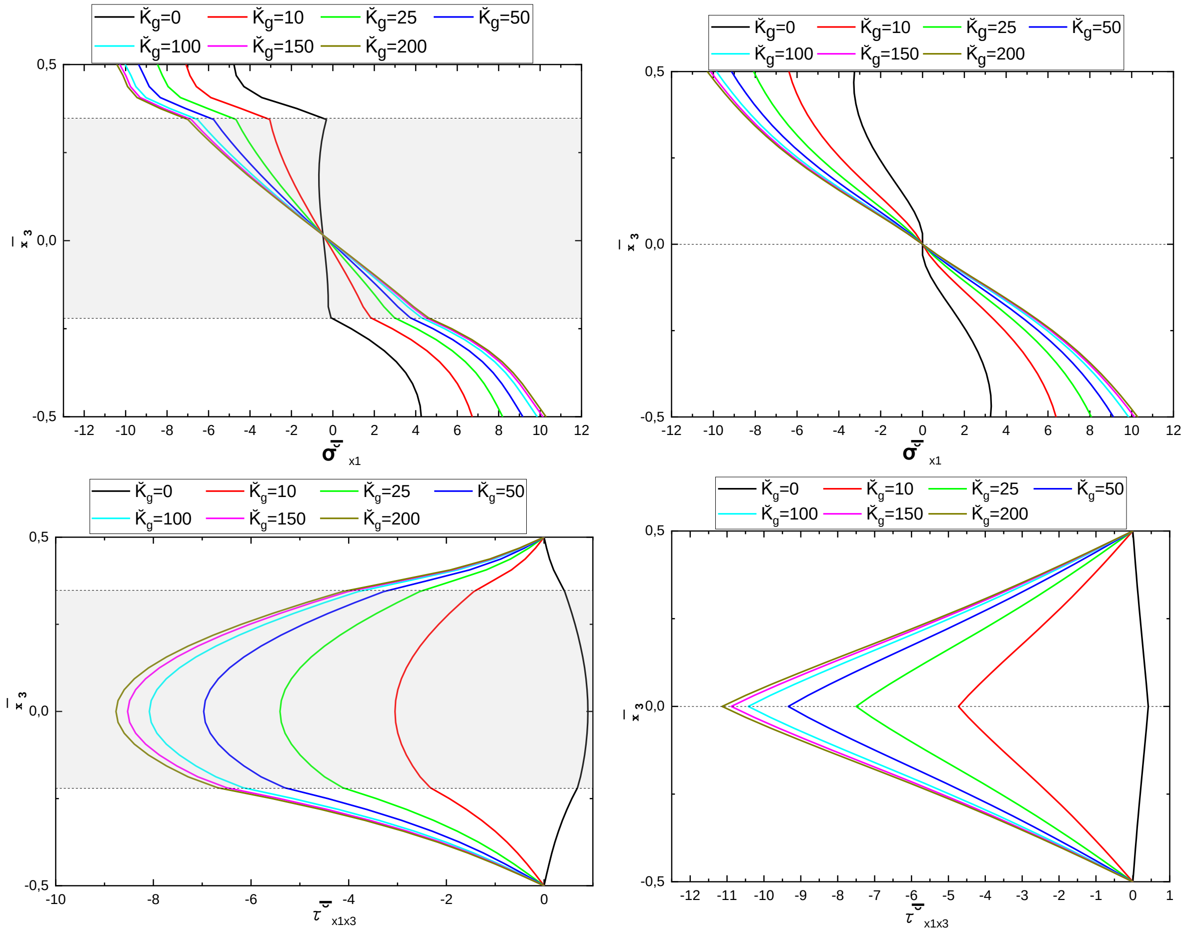

1-4-2 **1-0-1**

Fig 9: Variation of dimensionless stress $\bar{\bar{\sigma}}_{x_1}$ and $\bar{\bar{\tau}}_{x_1x_3}$ with $\bar{x}_3$ for two types of FGM sandwich plate under different value of shear layer foundation stiffness($\breve{t}_2 = \breve{t}_3 = 10, \breve{c}_2 = \breve{c}_3 = 100, \breve{t}_1 = \breve{c}_1 = 0, \breve{K}_w = 50, r = 2$)

It can be seen from Figure 8-9 for small values of the foundation parameters $\breve{K}_G$, $\breve{K}_w$, the dimensionless shear stresses $\bar{\bar{\tau}}_{x_1x_3}$ are positive and decrease as these parameters increase, and they continue to decrease until they become negative.

Additionally, it can be observed that the dimensionless stress $\bar{\bar{\sigma}}_{x_1}$and $\bar{\bar{\tau}}_{x_1x_3}$ curves converge in order to be large values of the foundation parameters $\breve{K}_G$, $\breve{K}_w$.

It can be seen from Figure 10-11 that an increase in hygro-thermal loads produces large values of dimensionless stress$\bar{\bar{\sigma}}_{x_1}$ and $\bar{\bar{\tau}}_{x_1x_3}$ in absolute terms. It is also noted that these dimensionless stress $\bar{\bar{\sigma}}_{x_1}$ and $\bar{\bar{\tau}}_{x_1x_3}$ are highly sensitive to thermal load versus moisture load, and this is by comparing Figure 10 with Figure 11.

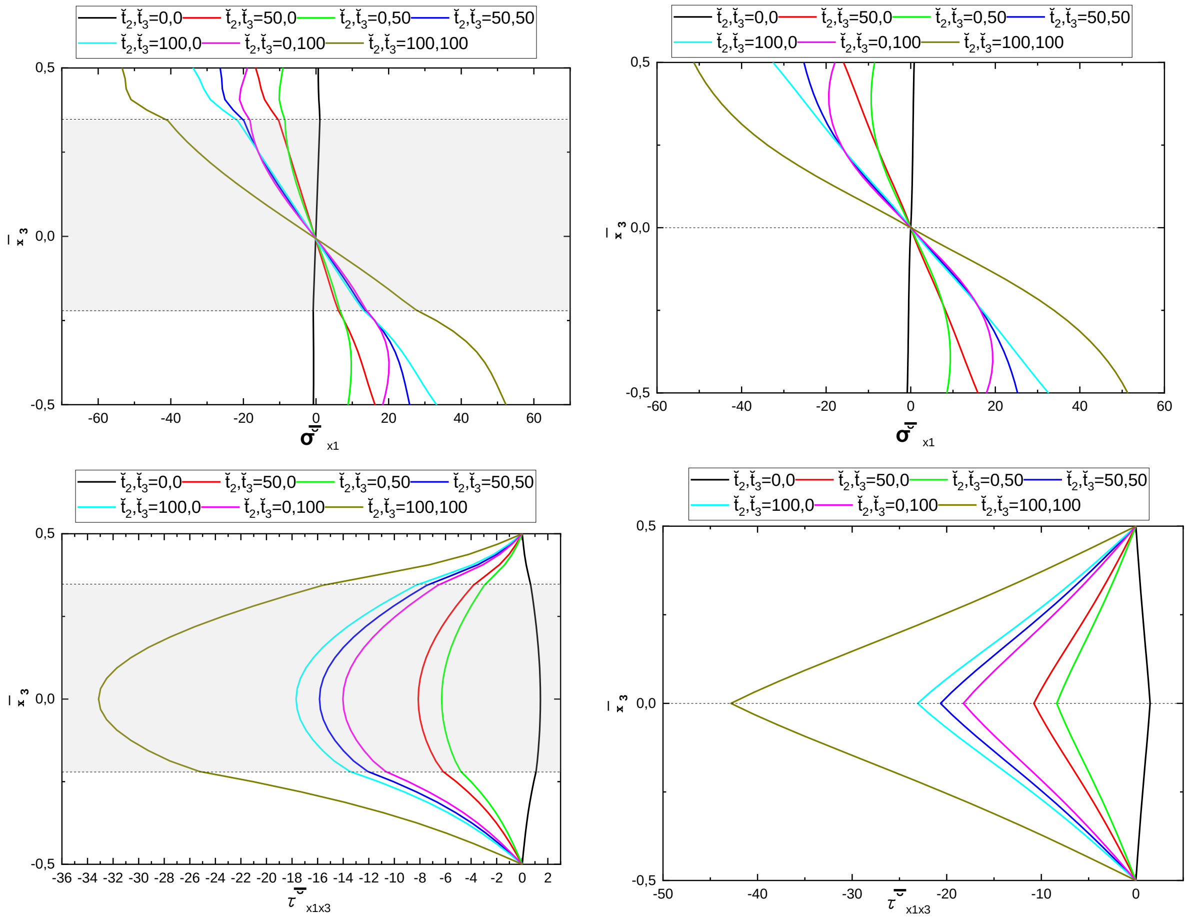

1-4-2 **1-0-1**

Fig 10: Variation of dimensionless stress $\bar{\bar{\sigma}}_{x_1}$ and $\bar{\bar{\tau}}_{x_1x_3}$ with $\bar{x}_3$ for two types of FGM sandwich plate under different value values of temperatures ($\check{c}_2 = \check{c}_3 = 10, \check{t}_1 = \check{c}_1 = 0, \check{K}_w = \check{K}_G = 10, r = 2$)

It can be seen from Figure 10-11 that an increase in hygro-thermal loads produces large values of dimensionless stress$\bar{\bar{\sigma}}_{x_1}$ and $\bar{\bar{\tau}}_{x_1x_3}$ in absolute terms. It is also noted that these dimensionless stress $\bar{\bar{\sigma}}_{x_1}$ and $\bar{\bar{\tau}}_{x_1x_3}$ are highly sensitive to thermal load versus moisture load, and this is by comparing Figure 10 with Figure 11.

It can be seen from Figure 11 that the effect of the values of the moistures C on the dimensionless stress $\bar{\bar{\sigma}}_{x_1}$ and $\bar{\bar{\tau}}_{x_1x_3}$ differs in central body of the plate versus in bodies on the surfaces of the plate represented by functionally graded materials and in the absence of middle core of the plate, that is in the case of 1-0-1 We also notice that the effect of the moistures C on dimensionless normal stress change between the central plane $\bar{x}_3$=0 and the extreme plane of the plate $\bar{x}_3 = \mp 0,5$, and this is after the curves intersect between them.

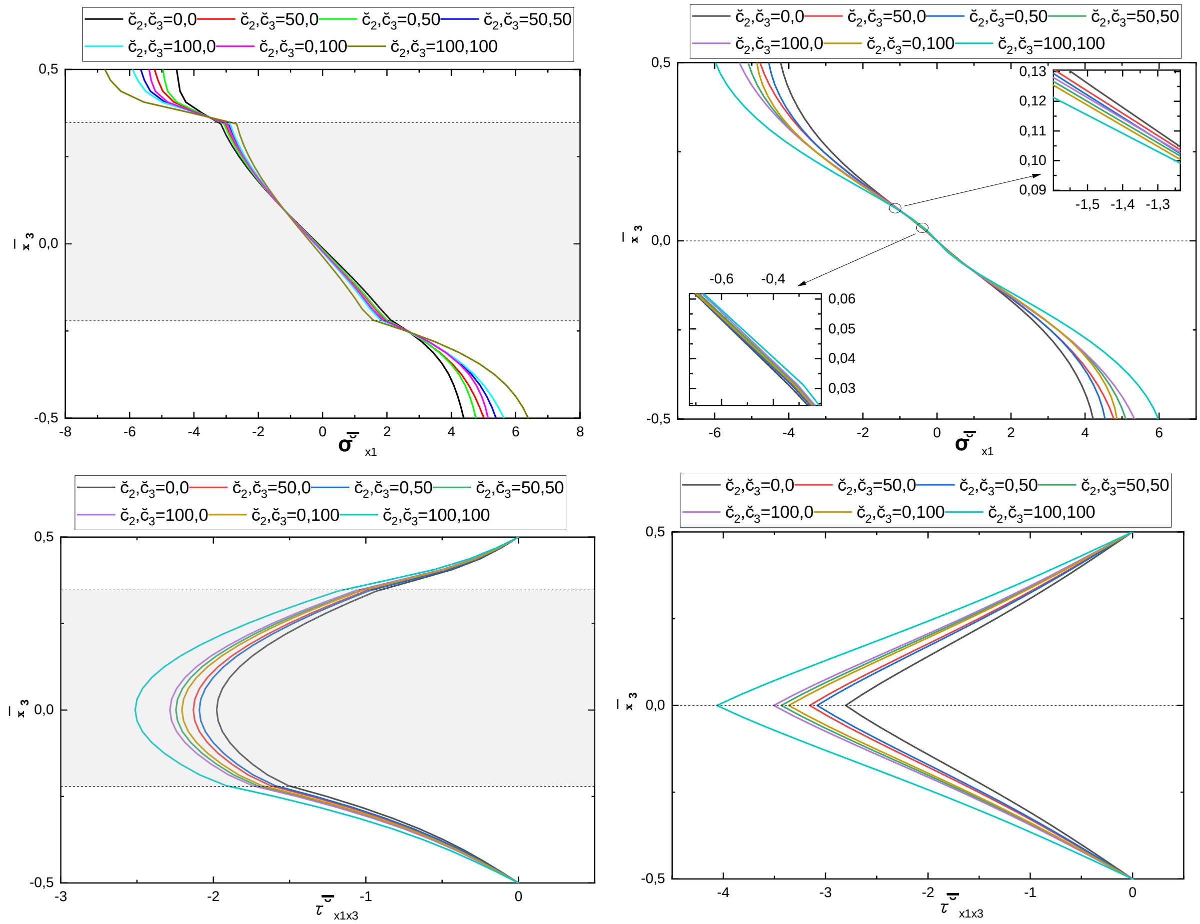

1-4-2 **1-0-1**

Fig 11: Variation of dimensionless stress $\bar{\bar{\sigma}}_{x_1}$ and $\bar{\bar{\tau}}_{x_1x_3}$ with $\bar{x}_3$ for two types of FGM sandwich plate under different values moistures. ($\check{t}_2 = \check{t}_3 = 10, \check{t}_1 = \check{c}_1 = 0, \breve{K}_w = \breve{K}_G = 10, r = 2$)

It can be seen from Figure 12 that the values volume fraction indices r has effect on the dimensionless stress $\bar{\bar{\sigma}}_{x_1}$ and $\bar{\bar{\tau}}_{x_1x_3}$ This effect is in a body on both surfaces of the plate represented by functionally graded materials.

In the case of a FGM sandwich plate without a middle core, the distribution of dimensionless shear stress $\bar{\bar{\tau}}_{x_1x_3}$ gradually changes in the central plan that ($\bar{x}_3$=0) when the volume fraction index s is smaller. On the other hand, the central plan ($\bar{x}_3$=0) distribution of dimensionless shear stress $\bar{\bar{\tau}}_{x_1x_3}$ varies greatly when the volume fraction index r is high.

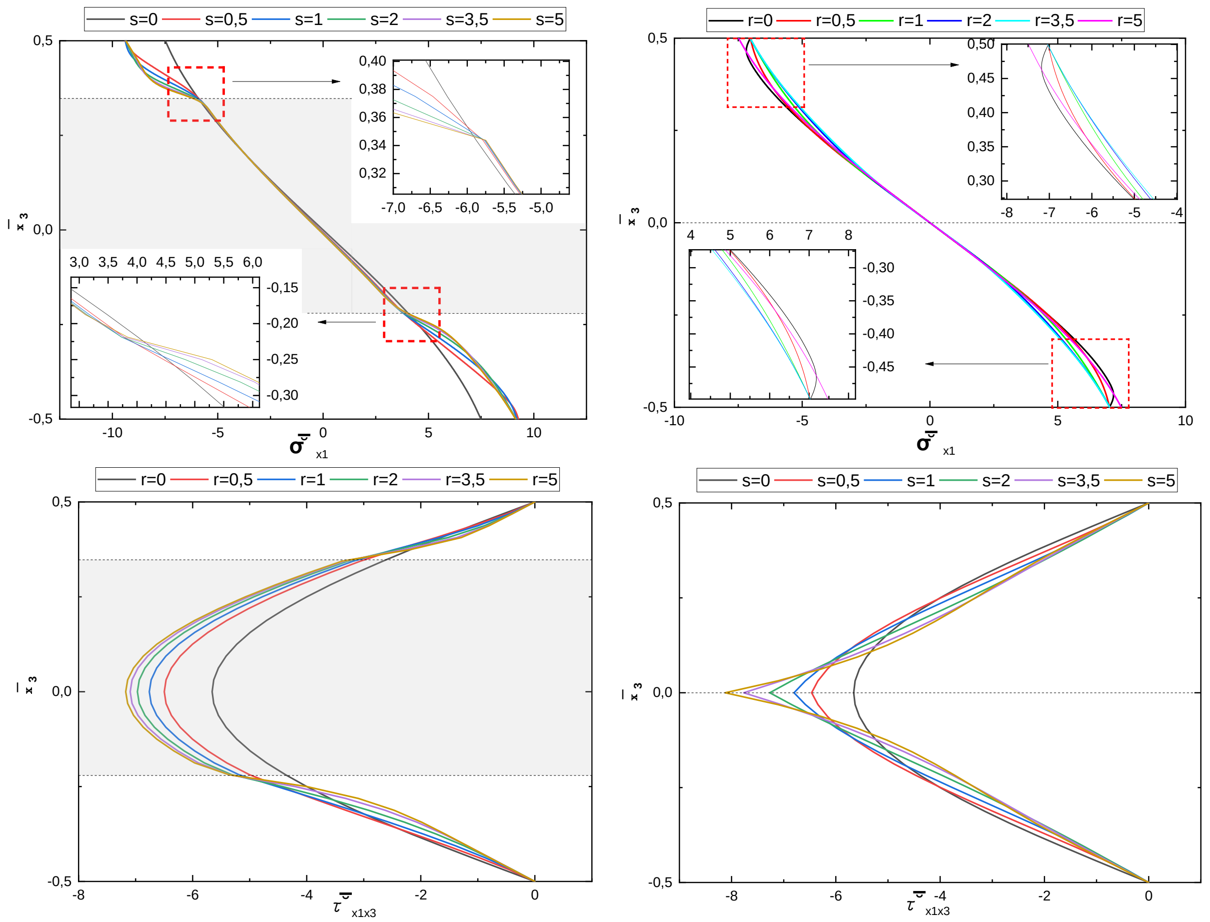

1-4-2 **1-0-1**

Fig 12: Variation of dimensionless stress $\bar{\sigma}_{x_1}$ and $\bar{\tau}_{x_1x_3}$ with $\bar{x}_3$ two types of FGM sandwich plate under different volume fraction indices s. ($\breve{c}_2 = \breve{c}_3 = \breve{t}_2 = \breve{t}_3 = 10, \breve{t}_1 = \breve{c}_1 = 0, \breve{K}_w = \breve{K}_G = 50$)

4. Conclusions

The bending of FGM sandwich plates under a hygro-thermo-mechanical load on two-parameter elastic foundations was analyzed using a four-variable refined plate model and refined trigonometric shear deformable plate theory. After applying the virtual work principle, the Navie solution was used to solve the equations.

The resulting solution was then used to investigate the effects of elastic foundation parameters, power-law index, loads, and the layer thickness ratio on deflection and stress.

We concluded that normal stress is greatest in boundary layers, while shear stress is greatest in central layers and decreases to zero in boundary planes.

In addition, the stress distribution is determined by the plate's symmetry. In the case of a symmetrical plate, the distribution of normal stress accepts a symmetry center, while shear stress accepts the symmetry axis. In asymmetrical panels, the normal and shearing stress curves are integrated through points of sympathy at each layer's extreme plane, resulting in a harmonious shape with all layers' thickness.

A plate without a central core with two equal layers is a special case of symmetric plate in which the stress distribution takes the distribution of two edge layers.

This research assists engineers in determining the shape of a FGM sandwich plate that can resist hygro-thermo-mechanical loads on structurally flexible foundations. Possibilities include symmetry, central core presence, and layer thickness.

References

[1] D. Feng, G. Loi, F. Aymerich, A Numerical and Experimental Investigation into the Impact Response of Sandwich Composites under Different Boundary Conditions, *Journal of Composites Science,* Vol. 6, No. 3, pp. 88, 2022.

[2] R. A. Alghanmi, R. H. Aljaghthami, A Four-Variable Shear Deformation Theory for the Static Analysis of FG Sandwich Plates with Different Porosity Models, *Mathematical and Computational Applications,* Vol. 29, No. 2, pp. 20, 2024.

[3] M. Koizumi, FGM activities in Japan, *Composites Part B: Engineering,* Vol. 28, No. 1-2, pp. 1-4, 1997/01//, 1997. en

[4] A. D. Kerr, Elastic and viscoelastic foundation models, 1964.

[5] T. A. Anderson, A 3-D elasticity solution for a sandwich composite with functionally graded core subjected to transverse loading by a rigid sphere, *Composite Structures,* Vol. 60, No. 3, pp. 265-274, 2003.

[6] H. H. Abdelaziz, H. A. Atmane, I. Mechab, L. Boumia, A. Tounsi, A. B. E. Abbas, Static Analysis of Functionally Graded Sandwich Plates Using an Efficient and Simple Refined Theory, *Chinese Journal of Aeronautics,* Vol. 24, No. 4, pp. 434-448, 2011/08//, 2011. en

[7] Q. Li, V. P. Iu, K. P. Kou, Three-dimensional vibration analysis of functionally graded material sandwich plates, *Journal of Sound and Vibration,* Vol. 311, No. 1-2, pp. 498-515, 2008/03//, 2008. en

[8] A. Keddouri, L. Hadji, A. Tounsi, Static analysis of functionally graded sandwich plates with porosities, *Advances in materials Research,* Vol. 8, No. 3, pp. 155-177, 2019/09/25/, 2019. en

[9] S. Merdaci, A. H. Mostefa, Influence of porosity on the analysis of sandwich plates FGM using of high order shear-deformation theory, *Frattura ed Integrità Strutturale,* Vol. 14, No. 51, pp. 199-214, 2019/11/25/, 2019. en

[10] B. Adhikari, P. Dash, B. N. Singh, Buckling analysis of porous FGM sandwich plates under various types nonuniform edge compression based on higher order shear deformation theory, *Composite Structures,* Vol. 251, pp. 112597, 2020/11//, 2020. en

[11] E. Njim, S. Bakhy, M. Al-Waily, Free vibration analysis of imperfect functionally graded sandwich plates: analytical and experimental investigation, *Archives of Materials Science and Engineering,* Vol. 111, No. 2, pp. 49-65, 2021.

[12] J. Liu, C. Hao, W. Ye, F. Yang, G. Lin, Free vibration and transient dynamic response of functionally graded sandwich plates with power-law nonhomogeneity by the scaled boundary finite element method, *Computer Methods in Applied Mechanics and Engineering,* Vol. 376, pp. 113665, 2021/04/01/, 2021. en

[13] N. Sharma, P. Kumar Swain, D. Kumar Maiti, B. Nath Singh, Vibration and uncertainty analysis of functionally graded sandwich plate using layerwise theory, *AIAA Journal*, Vol. 60, No. 6, pp. 3402-3423, 2022.

[14] H. Georges, G. Meyer, C. Mittelstedt, W. Becker, 2D Elasticity solution for sandwich panels with functionally graded lattice cores, *Composite Structures,* Vol. 300, pp. 116045, 2022.

[15] I. Benameur, Y. Beldjelili, A. Tounsi, Analytical and finite element method for the bending analysis of the thick porous functionally graded sandwich plate including thickness stretching effect, *Structural Engineering and Mechanics,* Vol. 85, No. 5, pp. 593-605, 2023/01/01/, 2023. en

[16] L. Kurpa, T. Shmatko, J. Awrejcewicz, G. Timchenko, I. Morachkovska, Analysis of free vibration of porous power-law and sigmoid functionally graded sandwich plates by the R-functions method, *Journal of Applied and Computational Mechanics,* Vol. 9, No. 4, pp. 1144-1155, 2023.

[17] K. Swaminathan, S. Hirannaiah, T. Rajanna, Vibration and stability characteristics of functionally graded sandwich plates with/without porosity subjected to localized edge loadings, *Mechanics Based Design of Structures and Machines,* Vol. 51, No. 11, pp. 6254-6292, 2023.

[18] P. Van Vinh, A. Tounsi, Free vibration characteristics of three-phases functionally graded sandwich plates using novel nth-order shear deformation theory, *Computers and Concrete,* Vol. 33, No. 1, pp. 27-39, 2024.

[19] L. Hadji, V. Plevris, R. Madan, H. Ait Atmane, Multi-directional functionally graded sandwich plates: buckling and free vibration analysis with refined plate models under various boundary conditions, *Computation,* Vol. 12, No. 4, pp. 65, 2024.

[20] Z. Huang, M. Han, X. Wang, F. Chu, Free Vibration of Functionally Graded Material Sandwich Plates with Soft Core, *Journal of Vibration Engineering & Technologies,* Vol. 12, No. 3, pp. 5119-5131, 2024.

[21] A. M. Zenkour, M. Sobhy, Thermal buckling of various types of FGM sandwich plates, *Composite Structures,* Vol. 93, No. 1, pp. 93-102, 2010/12//, 2010. en

[22] A. Tounsi, M. S. A. Houari, S. Benyoucef, E. A. Adda Bedia, A refined trigonometric shear deformation theory for thermoelastic bending of functionally graded sandwich plates, *Aerospace Science and Technology,* Vol. 24, No. 1, pp. 209-220, 2013, 2013.

[23] A. Benbakhti, M. B. Bouiadjra, N. Retiel, A. Tounsi, A new five unknown quasi-3D type HSDT for thermomechanical bending analysis of FGM sandwich plates, *Steel Compos. Struct,* Vol. 22, No. 5, pp. 975-999, 2016.

[24] D. Li, Z. Deng, G. Chen, H. Xiao, L. Zhu, Thermomechanical bending analysis of sandwich plates with both functionally graded face sheets and functionally graded core, *Composite Structures,* Vol. 169, pp. 29-41, 2017/06//, 2017. en

[25] S. J. Singh, S. P. Harsha, Thermo-mechanical analysis of porous sandwich S-FGM plate for different boundary conditions using Galerkin Vlasov's method: A semi-analytical approach, *Thin-Walled Structures,* Vol. 150, pp. 106668, 2020/05//, 2020. en

[26] A. A. Daikh, I. Bensaid, A. M. Zenkour, Temperature dependent thermomechanical bending response of functionally graded sandwich plates, *Engineering Research Express,* Vol. 2, No. 1, pp. 015006, 2020/01/06/, 2020. en

[27] S. Mahmoud, E. Ghandourah, A. Algarni, M. Balubaid, A. Tounsi, F. Bourada, On thermo-mechanical bending response of porous functionally graded sandwich plates via a simple integral plate model, *Archives of Civil and Mechanical Engineering,* Vol. 22, No. 4, pp. 186, 2022.

[28] M. Han, Z. Li, Z. Huang, X. Wang, W. Gao, Thermal Mechanical Bending Response of Symmetrical Functionally Graded Material Plates, *Materials,* Vol. 16, No. 13, pp. 4683, 2023.

[29] M. Han, J. Huang, Z. Huang, X. Wang, Bending Analysis of Asymmetric Functionally Graded Material Sandwich Plates in Thermal Environments, *Materials,* Vol. 16, No. 13, pp. 4682, 2023.

[30] S. Natarajan, G. Manickam, Bending and vibration of functionally graded material sandwich plates using an accurate theory, *Finite Elements in Analysis and Design,* Vol. 57, pp. 32-42, 2012.

[31] E. Reissner, On tranverse bending of plates, including the effect of transverse shear deformation, 1974.

[32] J. N. Reddy, A Simple Higher-Order Theory for Laminated Composite Plates, *Journal of Applied Mechanics,* Vol. 51, No. 4, pp. 745-752, 1984/12/01/, 1984.

[33] M. Touratier, An efficient standard plate theory, *International Journal of Engineering Science,* Vol. 29, No. 8, pp. 901-916, 1991/01/01/, 1991. en

[34] I. M. Mudhaffar, A. Tounsi, A. Chikh, M. A. Al-Osta, M. M. Al-Zahrani, S. U. Al-Dulaijan, Hygro-thermo-mechanical bending behavior of advanced functionally graded ceramic metal plate resting on a viscoelastic foundation, in *Proceeding of*, Elsevier, pp. 2177-2189.

[35] Y. Beldjelili, A. Tounsi, S. R. Mahmoud, Hygro-thermo-mechanical bending of S-FGM plates resting on variable elastic foundations using a four-variable trigonometric plate theory, *Smart Structures and Systems,* Vol. 18, No. 4, pp. 755-786, 2016/10//, 2016.

[36] D. Li, Z. Deng, H. Xiao, Thermomechanical bending analysis of functionally graded sandwich plates using four-variable refined plate theory, *Composites Part B: Engineering,* Vol. 106, pp. 107-119, 2016.

[37] A. A. Daikh, A. M. Zenkour, Bending of Functionally Graded Sandwich Nanoplates Resting on Pasternak Foundation under Different Boundary Conditions, *Journal of Applied and Computational Mechanics,* Vol. 6, No. Special Issue, 2020 décembre, 2020. en